Escola d'Enginyeria de Telecomunicació i Aeroespacial de Castelldefels

UNIVERSITAT POLITÈCNICA DE CATALUNYA

TREBALL FINAL DE GRAU

TÍTOL DEL TFG: Analysis of effect of large fuel tanks on aerodynamic performances of heavy trucks and large aircraft.

TITULACIÓ: Grau en Enginyeria d'Aeronavegació.

AUTORS: Edgar López i Xavier Paricio.

DIRECTOR: José Ignacio Rojas Gregorio.

DATA: 8/03/2017

TÍTOL DEL TFG: Analysis of effect of large fuel tanks on aerodynamic performances of heavy trucks and large aircraft.

AUTORS: Edgar López i Xavier Paricio

DIRECTOR: José Ignacio Rojas Gregorio

DATA: 8/03/2017

RESUM

En l'actualitat, el 90% de vehicles funcionen amb combustibles fòssils. L'ús de combustibles fòssils contribueix a l'efecte hivernacle i també a l'augment de contaminació arreu del món. L'hidrogen, es presenta com a una possible alternativa als combustibles fòssils.

De totes maneres, l'ús d'hidrogen com a combustible implica l'ús de tancs de combustible diferents. A causa de la seva baixa energia de densitat, l'hidrogen requereix tancs de combustible amb més volum que els combustibles convencionals, per mantenir una equivalència d'energia. Els tancs de majors dimensions, modifiquen la geometria externa del vehicle i per tant, l'aerodinàmica del vehicle també canvia.

L'objectiu d'aquest projecte és realitzar un anàlisi experimental i amb *Computational Fluid Dynamics* (CFD) d'un avió Airbus A320 i d'un camió cisterna on la seva geometria ha estat modificada tenint en compte l'augment dels tancs de combustible a causa de l'ús d'hidrogen com a combustible transportat. Aleshores, les prestacions aerodinàmiques dels vehicles modificats són comparades amb l'Airbus A320 convencional i el camió cisterna. El software utilitzat en aquest anàlisi és l'ANSYS Fluent. Com en altres anàlisis CFD, el procés que s'ha seguit consisteix en aquests passos: generació de la geometria, mallat, definició de les condicions de contorn i física del problema, càlcul i processat de resultats.

Primerament s'ha modelitzat el tanc de combustible del A320 i la cisterna del camió de forma que puguin emmagatzemar la mateixa quantitat de combustible que porten actualment i mantenir una equivalència d'energies. La modelització s'ha dut a terme pensant en el pitjor cas possible per l'aerodinàmica del vehicle.

A més a més, s'han escollit les dimensions del volum de control , és a dir, el camp d'actuació del fluid en el cos d'estudi. Les dimensions del volum de control han de ser suficientment grans per tal que la simulació no es vegi alterada.

ANSYS Meshing ens ha permès fer el mallat. S'ha intentat que les cel·les fossin el més refinades possible ens els llocs d'interès i que els paràmetres de qualitat de la malla com no es veiessin afectats greument de forma que els resultats siguin fiables.

Per a l'estudi de l'Airbus A320, s'han realitzat dues simulacions, una sense cap modificació i l'altre amb la modificació del tanc d'hidrogen com a combustible. Per l'estudi del camió cisterna, s'han realitzat tres simulacions, una sense cap modificació, una considerant que emmagatzema tot l'hidrogen en un sol tanc i l'última considerant que l'hidrogen és emmagatzemat en dos tancs per tal de millorar la maniobrabilitat del camió. La idea és poder comparar els resultats entre simulacions per poder entendre què està passant en cada vehicle.

S'ha vist que la modificació del A320 presenta un augment del drag i del lift. A causa de l' implementació del tanc d'hidrogen l'estructura de l'avió pesa més. Tot i això, com que ara el fuel és hidrogen i és més lleuger que el Jet A, el pes total es veu reduït. D'aquesta manera no necessitem volar amb cap angle d'atac superior ja que l'actual sustentació creada per l'ala ja és capaç de compensar el pes de l'avió. Tot i això, l'hidrogen és molt car actualment i la seva implementació seria molt costosa per les companyies aèries.
Pel que fa a les modificacions del camió cisterna, el camió format per dos tancs de combustible és el que presenta un major augment de drag. Tot i això no és gaire superior al que presenta un sol tanc de combustible. A causa de la millor maniobrabilitat creiem que és la millor opció.

Finalment hem imprès els prototips 3D de les geometries de l'avió estudiades i les hem analitzat en el túnel de vent per mesurar experimentalment les prestacions aerodinàmiques i comparar-les amb les obtingudes en les simulacions CFD. De l'anàlisi, es pot observar que hi ha molts factors externs que influeixen en la realització de l'experiment. De totes maneres, s'ha pogut veure com l'avió modificat presenta més drag a causa del tanc de combustible i l'eficiència també disminueix. D'altra banda, així com en les simulacions s'havia obtingut que hi havia més lift, ara el lift ha disminuït.

Finalment s'han redactat les conclusions i aspectes que han de ser considerats pel futur per tal de millorar o complementar el projecte.

TITLE OF THE TFG: Analysis of effect of large fuel tanks on aerodynamic performances of heavy trucks and large aircraft.

AUTHORS: Edgar López i Xavier Paricio

DIRECTOR: José Ignacio Rojas Gregorio

DATE: 8/03/2017

ABSTRACT

Nowadays, 90% of the worldwide vehicles work with fossil fuels. Use of fossil fuels contributes to the greenhouse effect and to increase the pollution worldwide. Hydrogen has been suggested as a possible alternative to fossil fuels.

However, the use of hydrogen as fuel implies using different fuel tanks. Due to its lower energy density, hydrogen requires fuel tanks with larger volume than conventional fuels, for an equivalent amount of energy released. The larger tanks modify the external geometry of the vehicle and therefore the aerodynamics are also different.

The aim of this project is to carry out an experimental and Computational Fluid Dynamics (CFD) analysis of an Airbus A320 and a tanker truck for which the geometries have been modified accounting for the larger hydrogen fuel tanks needed. Then, the aerodynamic performances of the modified vehicles are compared with the reference conventional A320 and tanker truck. The software used in this analysis is ANSYS Fluent. As in other CFD analysis, the procedure we followed consisted of these steps: generation of the geometry, meshing, definition of the boundary conditions and the physics of the problem, solving, processing of the results.

Firstly, the A320 and tanker truck fuel tank modelling have been done in order to stock up the same quantity of fuel as before and to keep an equivalent energy. The modelling process has been performed thinking about the worst possible aerodynamics case.

Furthermore, the control volume dimensions have been chosen, that is, the fluid field domain around the target body. Dimensions of the control volume have to be sufficiently big in order to not disrupt the simulation.

ANSYS Meshing allowed us to do the mesh. We have tried that cells were refined as much as possible into the interest zones. The mesh quality parameters have been considered to ensure that the simulation is reliable.

For the Airbus A320 study, two simulations have been carried out, the first one without any modification and the second one considering the implementation of hydrogen as fuel. For the tanker truck study, three simulations have been carried out, the first one without any modification, the second one considering that is constituted by one single hydrogen tank and the last one considering that is constituted by two hydrogen tanks in order to improve the manoeuvrability. The idea is to compare the simulations to better understand what is happening in each vehicle.

It has been seen that the modified A320 presents an increase on drag and lift forces. To be able to overcome this increase on drag, extra fuel will be burnt. Furthermore, because of the implementation of the hydrogen tank, the aircrafts structure weights more than before. However, as hydrogen is now the fuel and it weighs less than Jet A, the total weight of the aircraft is reduced. In this way, we do not need to fly with any AOA higher than the actual one because the current lift is able to compensate the weight of the aircraft. Pitifully, hydrogen is so expensive at present day, and its implementation would be very expensive for airlines.
Regarding the tanker truck modifications, the tanker truck constituted by two hydrogen tanks presents the higher increase on drag. However, is not too much larger than the one single hydrogen tank tanker truck. Because of the higher manoeuvrability, it is thought that it would be the best option.

We printed 3D models of the A320 studied geometries and tested them in a wind tunnel to measure experimentally the aerodynamic performances and compare them with the results of the CFD simulations. From this analysis, appears that there are many external factors that affect the experiment. However, it has been seen that the modified aircraft presents more drag because of the new fuel tank and the efficiency also diminishes. On the other hand, in the simulations more lift was created, in contrary, the lift has decreased in the wind tunnel test.

Finally, conclusions and future work have been written with the purpose of improving or complementing this project.

A en José I. Rojas,
pel seu interès, ajuda i implicació en aquest projecte.

A en Carlos Sánchez,
per l'ajuda i facilitació de dades en camions i combustibles.

A Siddharth,
per l'ajuda i facilitació de informació en adhesius.

A les famílies Paricio Vallespi i López Castillo,
pel constant suport i ànims durant la realització del projecte.

TABLE OF CONTENTS

LIST OF FIGURES

LIST OF TABLES

INTRODUCTION

The Earth's climate has changed throughout history. There have been cycles of glacial advance and retreat and small climate changes due to variations in the Earth's orbit (and therefore variations in the energy input by the Sun) and other factors.

Nowadays, the Earth's climate is changing significantly and rapidly because of the human impact and not for natural reasons like in the previous cases. Global warming is increasing due to greenhouse gases (GHG) emitted by factories, vehicles...

In order to reduce the GHG emissions, companies are developing new ways of producing energy (renewable energies), new systems able to work without fossil fuels, etc. Use of electric vehicles is one of the most developed ideas but may not be the best. In relation to eco-friendly combustion vehicles, hydrogen seems to be a good candidate as a fuel, since it accomplishes all the necessary. However, it presents some drawbacks like storage due to its low density and its expensive production cost.

The aim of this project is to study the implementation of hydrogen as fuel in a tanker truck and in an Airbus A320, from the perspective of the impact on the aerodynamic performances of these vehicles due to the larger tanks needed. Both, vehicles continuously working and consequently emitting GHG.

This project starts with some concepts about the hydrogen properties, also its production, distribution and storage. This chapter is created in order to familiarize with hydrogen as fuel and to provide its advantages and drawbacks.

The next chapter introduces you to some fundamentals of aerodynamics needed to follow this project. Besides, different types of wind tunnels are presented to better understand the experimental analysis.

Once the theory necessary to understand this project has been explained, Chapter 3 contains all the information about performing the simulations needed to obtain the results for each vehicle. The geometry, Mesh, setup and solution steps are explained with many details.

Chapter 4 contains all the graphical and numerical results from the simulations. The results are analyzed and conclusions are extracted.

Finally, Chapter 5 consists on explaining the experimental analysis. Furthermore, a simulation in ANSYS Fluent is done to compare the results obtained in the wind tunnel. To sum up the project, conclusions and possible future analysis are going to be explained.

CHAPTER 1. HYDROGEN AS FUEL

1.1. Background.

Since the beginning of the industrial era, human activity has been polluting significantly the world by means of emissions of several polluting agents, including GHG like CO_2, CH_4.... The levels of GHG have increased and decreased significantly many times since the formation of the Earth, but never in such a short period of time, geologically speaking, like the recent increase of anthropogenic nature. Hence, the global Earth's temperature has increased in parallel considerably in a very short period of time also.

Humankind has realized about the potential consequences of the increasing global warming and has called this phenomenon climate change.

Climate change is visible for all of us. We have seen that average and peak temperatures have increased in the last years, reaching records one after another. Besides, the rainfall regimes are changing in any geographical zones, and extreme meteorological phenomena are increasing in frequency and intensity around the world [1].

Ice layers and glaciers are currently melting at a fast rate due to the unusually high temperatures registered in the Poles, etc. This enormous quantity of melted water could increase the sea level, alter ocean water salinity, distort oceanic currents and therefore climate could change drastically, as well as flora and fauna. However, the question is: should we be concerned about the climate change? And the answer is, obviously, yes.

Then, what should humankind do? Stop emitting GHG, for instance. All vehicles are still mainly working with fossil fuels and emitting CO_2. In this section, hydrogen is studied as an alternative fuel to substitute fossil fuels like gasoline. Advantages and drawbacks, costs and production are shown.

1.2. What is hydrogen?

Hydrogen is a chemical element with chemical symbol H and atomic number 1. It is the lightest element in the periodic table and it is also the most abundant chemical element in the universe. The most common place to find hydrogen on the Earth's crust is in the water, since water molecules have two hydrogen atoms. This means that there is a lot of hydrogen in the Earth, because in the Earth's surface there are large quantities of water!

Another factor that makes hydrogen very interesting for the transport sector, is it its high combustion power. For instance, the main cryogenic engines of the Orbiter (space shuttle), the Ariane 5 and basically the most current large rocket launchers, burn hydrogen with oxygen.

Table 1.1 Comparison between Jet A1and hydrogen properties.

NAME	PHASE	DENSITY [kg/L]	SPECIFIC ENERGY [MJ/kg]
Hydrogen	Liquid	0.0708	141.9
Jet A1	Liquid	0.804	42.8

1.3. Hydrogen production methods.

Hydrogen in molecular form can be produced from many different sources, and in many different ways. The study of hydrogen extraction methods is especially interesting for the reasons mentioned above. We are able to extract hydrogen from hydrocarbons, which include GHG, but also from biological materials like water. Each process has its own advantages and drawbacks as discussed below.

1.3.1. Steam Methane Reforming (SMR).

Steam methane reforming (SMR) is the process by which natural gas or another methane stream is forced to react with steam (water vapour) in the presence of a catalyst to produce hydrogen and carbon dioxide [2]. The efficiency is about 72% in producing hydrogen.

As seen in the chemical production process below, this process uses smaller amounts of methane combined with water vapour to produce carbon monoxide and hydrogen. Therefore, GHG are emitted.

$$CH_4 + H_2O \rightarrow CO + 3H_2$$

1.3.2. Electrolysis of water.

Electrolysis is the process by which water molecules are split directly into hydrogen and oxygen molecules using electricity and an electrolyser device. The electrolysis reaction produces pure oxygen and pure hydrogen [3].

1.3.3. Gasification of coal and other hydrocarbons.

Hydrogen can be produced from a large range of hydrocarbon fuels, including coal, heavy residual oils, and other low-value refinery products. The hydrocarbon fuel is forced to react with oxygen in a less stoichiometric ratio, yielding a mixture of carbon monoxide and hydrogen [4].

1.3.4. Hydrogen from biomass.

Biomass conversion technologies can be divided into thermo-chemical and biochemical processes. The former produce hydrogen rich streams of gas a known as “syngas” (a blend of hydrogen and carbon monoxide) [5].

1.4. Costs.

As seen before, there are several methods of producing hydrogen. In this section, costs of these hydrogen production methods are discussed. It is important to highlight that the cleanest production methods are also the most expensive [6].
Namely, it is easy to see that electrolysis does not involve GHG emissions to produce hydrogen, and thus it is classified as eco-friendly. Despite being the eco-friendliest process, it is very slow and also expensive due to the amount of electricity needed.

Regarding SMR, there is a feedstock of around 2-5$ per kilogram. The delivered costs are about 1.60$ per kilogram [7].

Based on estimated cost ranges by the National Academy of Sciences and the US department of energy, different kinds of electrolysis methods would produce hydrogen at delivered costs of 6-7$ per kilogram on average. Obviously, this cost may vary depending of the electrolysis method. For instance, for the most expensive method, solar hydrogen production, the costs would be about 10-30$ per kilogram [8].

Regarding the gasification of coal and other hydrocarbons, hydrogen can be produced from coal gasification at delivered costs of about 2$ per kilogram [9]

Finally, we can use different methods for distributing the hydrogen produced from a biomass source, like for electrolysis. For example, using a liquid distribution by a tanker truck, the cost would range around 5-7$ per kilogram. There are more types of hydrogen production methods, but they need to be scaled to be able to produce in larger quantities in order to reach lower costs.

Table 1.2 Comparison of methods for producing hydrogen, considering criteria like the costs and impact to the environment.

METHOD	AVERAGE COST [$/kg]	ECO-FRIENDLY
SMR	2.63	NO
ELECTROLYSIS	7.26	YES
GASIFICATION	1.82	NO
BIOMASS	5.1	YES

As we can see, there are several methods of producing hydrogen easily and at a reasonable cost. However, some of these techniques involve emission of GHG when producing hydrogen, so again we would be polluting if using those

techniques. Basically, electrolysis and biomass hydrogen production methods are the eco-friendliest but pitifully they are also the most expensive.

1.5. Storage.

Hydrogen is the gas with highest thermal conductivity, and lowest viscosity and density. Due to these properties, hydrogen is the gas with highest probability of leaking (this is one of the reasons why its distribution is troublesome), and it is also highly flammable and volatile [10].

Hence, hydrogen has to be treated with great safety. Distribution and storage system have to be designed with the minimum risk of leakage and have to be checked regularly. However, hydrogen is not more dangerous than other fuels. The table 1.3 shows a comparison between the properties of some common gases used also as fuels.

Table 1.3 Comparison between properties of different gases [11].

PROPERTY	HYDROGEN	METHANE	PROPANE
Density [Kg/m^3]	0.084	0.717	2.01
Ignition temperature [^{o}C]	500	455	493
Minimum energy of ignition in air [MJ]	0.02	0.3	0.26
Volume for detonation in air %	18%	6.3%	1.1%

It is easy to see that the major problem with hydrogen storage is the very low energy required for its ignition with air. However, hydrogen needs much more volume concentration than the other gases for its detonation in air and also it has the major ignition temperature.

Hydrogen has an invisible flame when burning and, of course, this is also a problem when trying to detect a potential accident. Because of its low density, it disperses very fast and that is fortunately a point in favour for hydrogen to avoid dangerous gas accumulation.

1.5.1. Storage as a compressed gas.

Storing hydrogen as compressed gas is the easiest method and also the most extended to store small quantities of hydrogen.

In this method, hydrogen is contained in pressurized metallic cylinder, but the metal has to be chosen carefully. Hydrogen is composed by small molecules; they move rapidly and are able to diffuse inside materials that are impermeable to other gases. Diffusion of atoms can also happen inside the material and therefore affecting the mechanic behaviour of the material [12].

As said before, due to the low density of hydrogen, a leak could generate very high forces while exhausting the gas and thus transforming the pressurized container into a missile and maybe causing damage.

1.5.2. Storage as a cryogenic liquid.

This is actually the unique method to store a large amount of hydrogen. A cryogenic liquid is called the gas that has been cold until transforming into a liquid phase. There are some problems related to the cryogenic hydrogen.
The human skin is easily frozen when in touch with cryogenic surfaces. Thus, all pipelines have to be isolated. Besides of preventing human accidents, also the isolation is needed in order to prevent the condensation of the air surrounding the pipelines that could generate a dangerous explosion if the liquid air is mixed with the nearly fuels [13].

However, liquid hydrogen is safer than gaseous hydrogen. In case of a structural failure of similar failures, liquid hydrogen would remain inside the container while in gaseous phase it would not.

1.6. Distribution.

Despite the advantages of hydrogen (for example, it is a good fuel in order to reduce GHG emissions), it has several distribution problems.

That is why, currently, the delivery costs of hydrogen are much more expensive than those for gasoline. Therefore, hydrogen is actually feasible and cost-effective only if produced and used near the place where it has to be used. Thus, for instance, since its distribution is so complicated, hydrogen would be very useful for powering vehicles.

Building a global distribution pipeline network has been suggested, but to build it a large investment is needed [14]. Due to the lack of funding money, the re-utilization of the actual gasoline or natural gas pipeline network seems to be the best idea.

1.7. Summary

In this section we have seen the motivation and drawbacks for using hydrogen as fuel in large vehicles. Combustion of hydrogen does not emit GHG and makes it an eco-friendly fuel. Therefore, for vehicles like an aircraft or a truck (storing hydrogen in a compressed gas or cryogenic liquid form) that have to travel along large distances it would be very interesting to reduce emissions and consequently, the pollution.

However, due to its low energy density, the volume that occupies hydrogen is much bigger than using a conventional fuel like gasoline. Hence, if we want to keep the equivalent energy, bigger fuel tanks are needed but can modify the aerodynamics performance of the vehicle. The change on the aerodynamics of the vehicle could provoke significant variations on other parameters like the efficiency. This study will be carried out in the subsequent chapters in order to determine the benefits-costs of implementing hydrogen as fuel.

CHAPTER 2. FUNDAMENTALS OF AERODYNAMICS

2.1. Classification of fluid flow

This section is intended to present the different types of flows that could be involved in aerodynamics, according to various criteria. The section focuses already in concepts particular to the proposed project. Thus, allusions are continually made to the simulations that will be carried out later on.

2.1.1. Incompressible versus compressible flow

A compressible flow is that for which the fluid density ρ varies significantly within the flow field. On the other hand, an incompressible flow is that for which the density ρ remains constant.

For instance, in this project we will analyze an aircraft flying at an altitude of 11 km at its cruise speed but also a truck at sea level (SL) moving at 80km/h. Depending on the value of the Mach number (that is, the ratio between the velocity at which the vehicle is moving through the air V, and the speed of sound, V_{sound}). We may be able to treat the airflow as incompressible or not.

The Mach number, *M*, (see Mach regimes in Table 2.1) can be calculated as:

$$M = \frac{V}{V_{sound}}$$

$$V_{sound} = \sqrt{\gamma R' T}$$

Where γ is the adiabatic constant, R' is the Universal constant of perfect gases particularized for the fluid under study and T is the temperature.

Table 2.1 Flow regimes depending on the Mach number.

REGIMES	MACH NUMBER	FLOW SITUATION
Incompressible	M<<1 (M<0.3)	Incompressible
Subsonic	M<1	Compressible
Transonic	M≈1	Compressible
Supersonic	M>1	Compressible
Hypersonic	M>>1	Compressible

Since for the A320 aircraft the simulation will be carried out at flight level (FL) 110 (11000 ft) and supposing that it is flying at cruise speed, (828 km/h):

$$M_{A320} = \frac{230\ m/s}{294.88\ m/s} = 0.78$$

On the other hand, the truck will be moving at SL at a velocity of 80 km/h. Thus:

$$M_{Truck} = \frac{22.22\ m/s}{340.08\ m/s} = 0.065$$

Table 2.2 below shows the conclusions as per the Mach regime:

Table 2.2 Fluid flow depending on Mach number results.

Vehicle	Mach number	Flow regime	Flow condition
Aircraft	0.78	High subsonic	Compressible
Truck	0.065	Low subsonic	Incompressible

2.1.2. Laminar versus turbulent flow

Laminar flow is when a fluid flows in parallel layers, with no disruption between the layers (see Fig.2.1). In laminar flow, the motion of the particles of the fluid is very orderly with particles close to a solid surface moving in straight lines parallel to that surface. Laminar flow generally occurs when the fluid is moving slowly or the fluid is very viscous. At higher velocities, the flow will transition from laminar to turbulent and therefore they Reynolds number will increase.

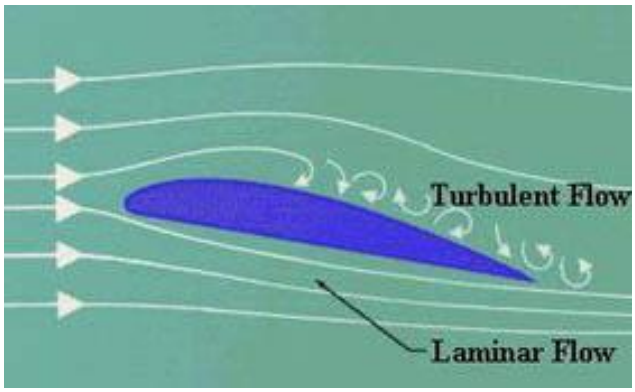

Fig. 2.1 Turbulent flow versus laminar flow due to the existing differential velocities.

In order to classify our fluid as turbulent or laminar we need to compute the Reynolds number, Re :

$$Re = \frac{\rho V d}{\mu} = \frac{uL}{\nu}$$

Where d is a characteristic dimension of the fluid problem, μ is the dynamic viscosity, L is the characteristic length and ν the kinematic viscosity. As we will analyze a real situation in which the flow moves around the vehicle (external flow simulations), the flow will be considered as turbulent if the Reynolds number is higher than 10000, as shown in Table 2.3

To proof the turbulent flow, the Reynolds number computation is shown below:

$$Re_{A320} = \frac{230 \cdot 37.43}{3.89 \cdot 10^{-5}} = 221 \cdot 10^{6} \gg 10000$$

$$Re_{Tanker\ truck} = \frac{22 \cdot 14.42}{1.51 \cdot 10^{-5}} = 21 \cdot 10^{6} \gg 10000$$

Table 2.3 Classification of the flow depending of the Reynolds number [15].

Type of flow	Reynolds interval
Laminar flow	Re<2000
Transitional flow	2000<Re<10000
Turbulent flow	Re>10000

2.1.3. Steady versus unsteady flow

For a fluid flow, a set of fluid properties can be identified, like the velocity field or the pressure field. If a flow is such that the fluid properties at every point in the fluid domain do not depend upon time, it is called steady flow.

On the contrary, if a flow is such that its fluid properties at every point in the flow domain do depend on time, it is called unsteady flow.

The simulations that have been done in this project consider the flow as steady since all the fluid properties are considered to remain constant with time in the truck and aircraft in the cruise conditions and rectilinear movement.

2.1.4. Newtonian vs. non-Newtonian flow

A Newtonian fluid is the fluid whose viscosity remains constant, no matter the amount of shear applied for a given temperature, that is, a fluid for which its viscosity depends on the local temperature and pressure, while it is independent of the deformation rate. These fluids have a linear relationship between viscosity and shear stress. On the other hand, non-Newtonian fluids are the opposite of Newtonian fluids: their viscosity depends also on the deformation rate. Hence, in our case the fluid is air and is considered a Newtonian fluid.

2.2. Aerodynamic forces

Aerodynamic forces appear when a body is moving through a fluid: air in this case. In this project, we have an aircraft and a truck moving through the air, so they will experience aerodynamic forces: lift and drag (see Fig.2.2).

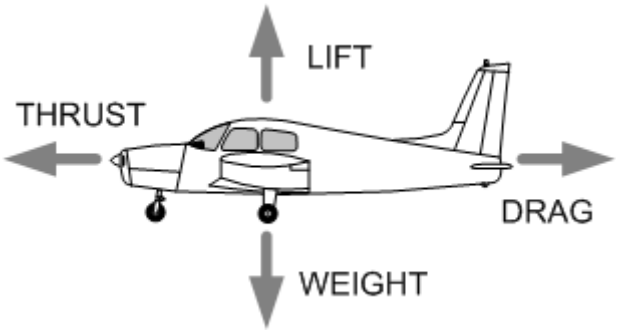

Fig. 2.2 Aerodynamic forces in flight

2.2.1. Lift

As we can see in Fig2.2, the lift is the component of the aerodynamic force perpendicular to the incident flow. For an aircraft, this component counter-balances the weight in horizontal flight condition. It is the responsible of keeping the aircraft in the air without falling down. The lift can be calculated as follows:

$$L = \frac{1}{2}\rho S V^2 C_L$$

Where S is a reference area (for instance, the wing layout area in the case of the aircraft) and C_L is the lift coefficient.

The lift coefficient is a dimensionless parameter that establishes how good is a vehicle at creating lift, irrespective of its size, velocity and atmospheric or tests conditions.
It depends basically on the shape/geometry of the vehicle, and its angle of attack (see Fig.2.3), although, it is true that, in reality, it depends also on the flow conditions (the Reynolds and Mach numbers). It is seen that:

$$C_L = \frac{2L}{\rho V^2 S} = \frac{L}{qS}$$

That is, the lift coefficient is the ratio between the lift force to the force produced by the dynamic pressure times the surface of the object that is producing the lift. Looking at Fig.2.3, we can see that the lift force depends on the angle of attack of the body respect to the fluid.

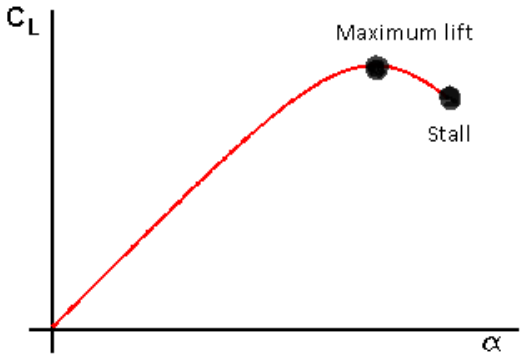

Fig. 2.3 Lift coefficient versus angle of attack

2.2.2. Drag

Looking again at Fig 2.2 we can see that the drag is the component of the aerodynamic force aligned with the incident flow. This component opposes the motion of the vehicle, and thus, unless counterbalanced by some sort of thrust or traction force, it would cause the vehicle to decelerate. The drag can be calculated as follows:

$$D = \frac{1}{2}\rho S V^2 C_D$$

In this case, the drag coefficient C_D is another dimensionless parameter that measures how good is a vehicle at creating drag, irrespective of its size, velocity and atmospheric or tests conditions. It is more difficult to estimate than the lift coefficient due to the multiple existing sources of drag.

Namely, the sources of drag are:

- **Form drag or pressure drag:** This type of drag is caused by the separation of the boundary layer from a surface and the wake created (see Fig.2.4). It is fundamentally caused by the shape or form of the aircraft.

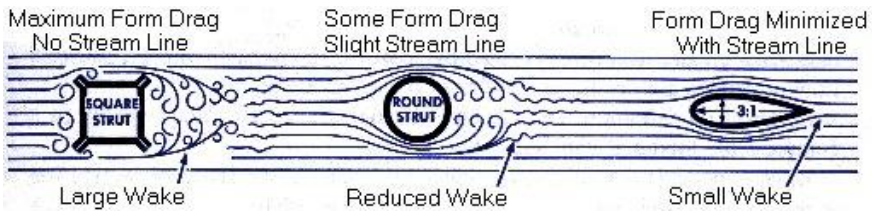

Fig. 2.4 Different shapes show the magnitude of form drag.

In Fig.2.4, airflow attempts to maintain contact with the surface of the square structure, but the streamlines are unable to follow the sharp angles. In consequence, they separate at the trailing edge leaving a low pressure wake

behind it. The difference of pressure between the leading and trailing edges of the square structure causes the structure to be pushed in the direction of the relative wind and retards forward motion due to the form drag [16].

- **Skin friction drag:** Friction drag is created in the boundary layer due to the viscosity of the air and the resulting friction against the surface of the aircraft. As the air flow molecules past the surface and past each other, the viscous resistance to that flow becomes a force which retards forward motion. Turbulent flow creates more friction drag than laminar flow due to its greater interaction with the surface of the airplane. This type of drag can be reduced delaying the point at which the laminar flow becomes turbulent. This can be accomplished by smoothing the exposed surfaces of the airplane by polishing or using flush rivets on the leading edges [17].

- **Interference drag:** This type of drag is generated when the airflow across one component of an aircraft like the wing or fuselage, is forced to mix with the airflow across and adjacent component.

- **Wave drag**: This type of drag appears on aircraft wings and fuselage, propeller blade tips and projectiles moving at transonic and supersonic speeds due to the presence of shock waves.

- **Induced drag:** This type of drag appears when a body is trying to redirect the airflow coming at it. This drag force occurs in an aircraft when redirecting the air to cause lift and also in cars when redirecting the air to cause a down force. This drag can be calculated as follows:

$$C_{D_i} = k \cdot C_L^2$$

$$k = \frac{1}{\pi \cdot AR \cdot e}$$

$$AR = \frac{b^2}{S}$$

Where AR is the aspect ratio, e the Oswald efficiency factor and b the wingspan.

- **Ram drag**: This type of drag appears in air-breathing engines (see Fig. 2.5) when air enters inside the aircraft engines for the combustion and therefore to produce thrust.

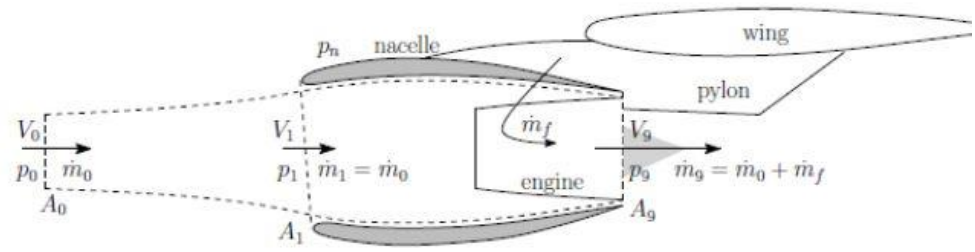

Fig. 2.5 Lateral view of an air-breathing engine and variables in various stages.

The net thrust can be computed as:

$$T = \dot{m}_9 V_9 - \dot{m}_0 V_0 + (p_9 - p_0)A_9 - (D_a + D_{pe} + D_{fe})$$

The term D_a is the additive ram drag and occurs in the inlet of the nozzle. Ram drag can be calculated as follows:

$$D_a = \int_0^1 (p - p_0)dA$$

In this study, the Airbus A320 is flying in cruise conditions. Ram drag can be cancelled with an adapted intake [18].

The previous types of drag can be distinguished between parasitic and non parasitic drag. Parasitic drag is a combination of interference drag, pressure drag and skin friction drag, while wave drag, induced drag and ram drag are not considered to be contributions to parasitic drag.

Fig.2.6 shows the behaviour of drag with airspeed in horizontal rectilinear flight condition: the parasitic drag increases with airspeed, while the induced drag decreases. It is important to remember that the angle of attack and speed have a relationship with the induced drag and parasite drag.

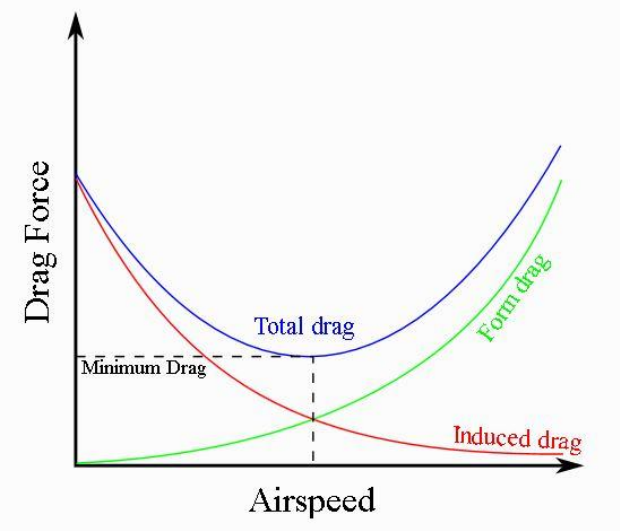

Fig. 2.6 Drag force versus true airspeed in uniform straight horizontal flight.

Occurs that when flying in horizontal condition, drag is balanced by thrust and therefore maximum velocity implies maximum drag. Moreover, increasing lift implies increasing drag. We can see that there is an important point called the minimum drag speed point. This point allows the aircraft to flight with an optimal velocity where lift is maximized and drag minimized and thus reducing fuel consumption. Therefore, this point can also be understood as the efficiency of the aircraft. Thus, a higher L/D ratio indicates an aircraft more efficient.

$$C_D = C_{D_0} + C_{D_i}$$

$$E = \frac{L}{D} = \frac{C_L}{C_D}$$

2.3. FUNDAMENTALS OF WIND TUNNEL TESTS.

Aerodynamic tunnels, also called wind tunnels, are scientific-technological instruments whose purpose is to study the behaviour of a fluid moving around and/or through an obstacle, and to measure the loads the fluid exerts on the obstacle.

In this project, the wind tunnel tests will provide information on how the airflow behaves in the proximities of the studied vehicles, the pressure distribution in these vehicles and the aerodynamic forces the fluid exerts.

2.3.1. Types of wind tunnels

Wind tunnels are often classified according to the flow speed in the test section relative to the speed of sound, that is, the Mach number in the test section. This way, wind tunnels are classified as subsonic, transonic, supersonic or

hypersonic (see Table 2.1). Compressibility affects the design of the test section of a wind tunnel: for subsonic tunnels, the test section has de smallest cross-sectional area of the tunnel; for supersonic tunnels, the test section area is chosen to achieve a desired Mach in the test section [19].
Wind tunnels can also be classified according to the geometry of the tunnel. For instance, typical subsonic wind tunnels are:

- **Open return tunnel or Eiffel tunnel:** This type of wind tunnel can have an open or a closed test section. The air coming from the room or the ambient passes through the test section and then is ejected back to the room as seen in Fig. 2.7. The open return tunnel has advantages and drawbacks:

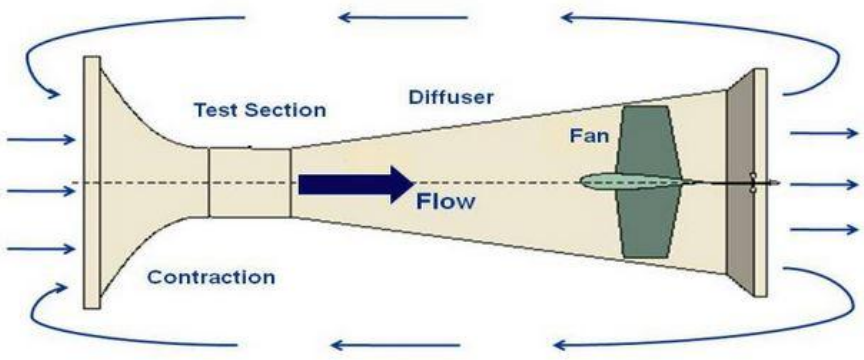

Fig. 2.7 Scheme of an open return wind tunnel.

Advantages:

1. Lower construction cost
2. There is no accumulation of exhaust products in an open tunnel

Disadvantages:

1. Poorer flow quality in the test section. The tunnel should be kept away from objects in the room in order to not disrupt the flow entering into the tunnel.
2. Higher operation costs. The fan must continually accelerate the flow.
3. Noisy operation.

- **Closed return wind tunnel or Prandtl tunnel.** In the closed return tunnel (see Fig. 2.8), the air is guided from the outlet of the test section back to its inlet thanks to a closed return circuit. This duct has a series of guided vanes in the elbows to minimize the pressure drops in these turns.

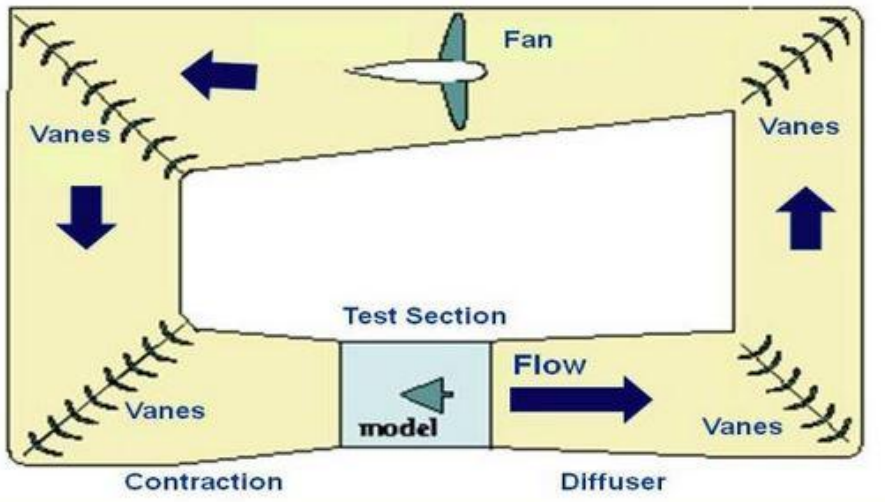

Fig. 2.8 Scheme of closed return wind tunnel.

2.3.2. Principle of similarity.

According to the dimensional analysis and similarity principles in fluid mechanics, a wind tunnel test with a scaled model of the structure requires the existence of geometric, kinematic and dynamic similarity between the flow around the scaled model and the flow around the real object, for the results in the tests to be directly valid for the real fluid problem.

I. Geometric similarity

Geometric similarity does not imply that the scaled model must be scrupulously equal to the real object. That is physically impossible in many cases due to the scales we manage. What is really important is to reproduce with high fidelity those features that are relevant to the aerodynamic performances.

II. Kinematics similarity

Two flows exhibiting similar streamlines satisfy the kinematics similarity principle. A requirement to have similar streamlines is that the conditions of the incident flow must be similar in both cases. For instance, the velocity profile and the turbulence of the incident in the scaled model should be similar to those of the incident flow in the real fluid problem.

III. Dynamic similarity

Dynamic similarity principle says that an easy relation must exist between the aerodynamic forces acting on similar bodies. This way; the aerodynamic coefficients measured for the scaled model in the wind tunnel tests will be the same as those for the real vehicle in the real fluid problem.

The validity of wind tunnel results obtained in testing of scale models is based on the fluid mechanics Principle of Dynamic similarity [20].

"If two physical phenomena or problems can be described using the same formulation (same equations and same initial boundary conditions), the solutions obtained for one of the phenomena are valid for the other one."

For the fluid motion around and an obstacle, this Principle ensures that the non-dimensional results measured in a wind tunnel for a scale model will be the same as for the real, full-scale obstacle if the following conditions are fulfilled:

- Geometric similarity: All relevant aerodynamic features of the real obstacle must be accurately replicated in the scaled model.
- The Mach number must be the same in both fluid problems.
- The Reynolds number must be the same in both fluid problems.
- Heat transfer (thermal effects) and diffusion can be neglected.

CHAPTER 3. CFD ANALYSIS.

In this Chapter we will explain the CFD analysis and the procedure we followed so that anyone can recreate our project with less difficulty than we had.

We take as a reference the CADs done in SolidWorks, so we can divide our study in two main blocks: one related to the analysis of the aircraft and another related to the analysis of the truck. In both cases, the objective is the same: to simulate the vehicles in the same conditions as in reality, and see how their aerodynamic performances are affected when we modify the vehicles.

To achieve that goal, we have to use a specific CFD program called ANSYS. When choosing the *Fluid Flow (Fluent)* module, we can see that we have four main steps to get the results of the simulation (see Fig. 3.1). We are going to explain in detail these steps for each simulation.

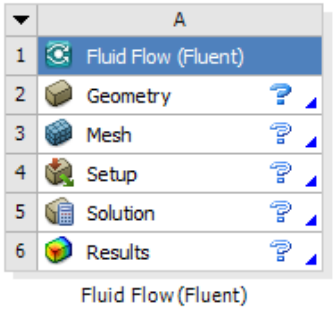

Fig. 3.1 Steps to be taken to perform the simulation in ANSYS Fluent.

3.1. Geometry.

In this section, modified geometries for the Airbus A320 and the tanker truck are proposed in order to account for the new larger fuel tanks needed to store the required hydrogen to maintain an equivalent energy as for the reference vehicles using conventional fuels.

The purpose of this chapter is not only to design the new fuel tanks capable of storing a specific amount of hydrogen, but also to put forward models in which the aerodynamic parameters can be affected strongly. Therefore, the designs presented here-in have been devised considering the worst case scenario for the aerodynamics of the vehicle.

Moreover, increasing the volume of the tank could also be important for a truck in which the dimensions are very regulated and constrained due to the roads in which it has to operate. Hence, the manoeuvrability is also an important parameter that has been considered.

3.1.1. Airbus A320 fuel tank.

At present day, the most common fuel in the air transport industry, and particularly in gas-turbine engines, is Jet fuel. This fuel is chosen because of many factors, for example, its higher flash point[1] and efficiency compared to other fuels [21].

However, in spite of being the most common fuel, this does not mean that it is the best according to some criteria. Namely, when burnt, Jet fuel is responsible for emissions of GHG and this should be prevented to mitigate climate change. Hydrogen has been proposed as an alternative fuel because its combustion has no associated emissions of GHG [22]. Since hydrogen has lower energy density, it is necessary to increase the volume of the fuel tank to maintain an equivalent energy as for the reference vehicles using conventional fuels.

This may entail a problem as it affects the aerodynamic performances of aircraft.

3.1.1.1. Specifications of the conventional A320.

The modified design of A320 that we propose has been calculated based on the actual dimensions of the conventional A320 aircraft and taking into account the factor that correlates the energy density of the Jet fuel and the hydrogen fuel. This way, we can make an approximation of the larger volume of the new hydrogen fuel tanks.

The actual dimensions of the conventional A320 (see Fig. 3.2) are as follows:

- Length: 37.57 m (123 ft 3 in).
- Wingspan: 35.8 m (117 ft 5 in).
- Tail height: 11.76 m (38 ft 7 in).
- Fuel capacity: 24210 L (standard), 30 190 (maximum).
- Cruising speed: 828 km/h (Mach 0.78) at 11 000 m.

[1] Flash point refers to the temperature at which the fuel will continue burning without and ignitions source, so the higher flash point of Jet Fuel makes it safer to transport and handle.

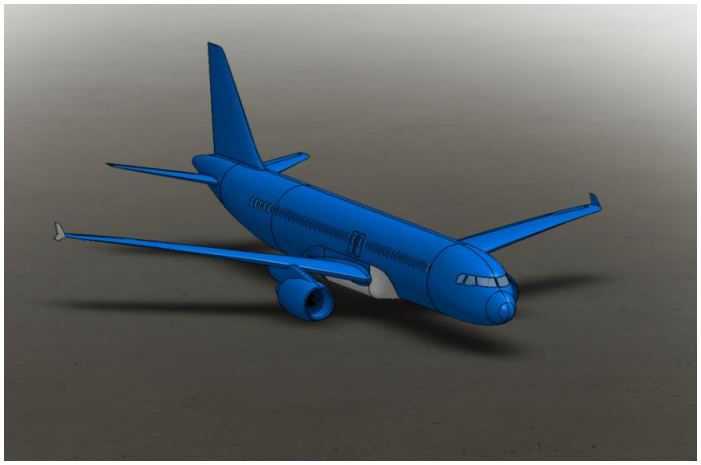

Fig. 3.2 Isometric view of a CAD design of a conventional Airbus A320 aircraft.

The most important of these specifications for the purpose of this study is the maximum fuel capacity: 30190 L or 30190 dm^3.

3.1.1.2. A320 Hydrogen tank design.

Next, we will model the necessary tank for hydrogen fuel. It will be ellipsoidal to fit better the modified aircraft. From the volume mentioned before, and the factor relating the energy densities of Jet fuel and hydrogen, we can calculate the volume of the new tank:

$$V_{Hydrogen} = 4 \cdot 30.19\ m^3 = 120.76\ m^3$$

We have decided to use an aircraft configuration with a single large fuel tank in its dorsal region with the volume just computed, and considering that the length of the modified A320 aircraft is also 37.57 m. A single tank has been established to be the best configuration because the more tanks the more wet area and thus the more friction aerodynamic drag. From the CAD of the conventional A320, we decided that the length of the new tank would be 18.71 m. Thus, the frontal area (or cross-sectional area) of our fuel tank would be:

$$Area_{Tank} = \frac{V_{Hydrogen}}{Tank\ Length} = 6.45\ m^2$$

We can calculate the area of an ellipsoid as:

$$Area_{ellipsoid} = \pi \cdot a \cdot b$$

$$Area_{Tank} = \frac{V_{Hydrogen}}{Tank\ Length} = \frac{120.76\ m^3}{18.71\ m} = 6.45\ m^2$$

With this expression, we will now calculate the area of the actual fuselage with the chosen design dimensions, as shown in Fig.3.3

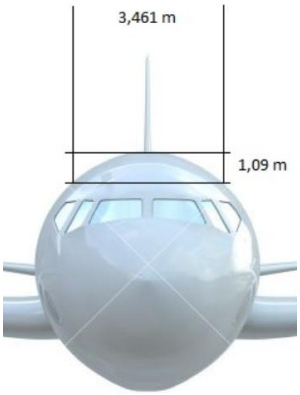

Fig. 3.3 Sketch of the frontal view of an aircraft.

$$b_{fuselage} = \frac{3.46\ m}{2} = 1.73\ m\ ;\ a_{fuselage} = 1.09\ m$$

$$Area_{fuselage} = \frac{\pi \cdot a_{fuselage} \cdot b_{fuselage}}{2} = 2.96\ m^2$$

With this, we can calculate the height of the new tank:

$$Area_{Tank} = Area_{ellipsoid} - Area_{fuselage}$$

$$Area_{ellipsoid} = \frac{\pi \cdot a_{Tank} \cdot b_{Tank}}{2}$$

$$b_{ellipsoid} = b_{fuselage}$$

$$a_{ellipsoid} = \frac{2 \cdot (Area_{Tank} + Area_{fuselage})}{\pi \cdot b_{fuselage}} = 3.46\ m$$

$$Height_{from\ fuselage} = a_{ellipsoid} - a_{fuselage} = 2.37\ m$$

The new fuel tank, modelled as an ellipsoid, will raise 2.37 m above the actual fuselage. The decision of designing the tank this way is giving an easy update to hydrogen fuel for actual aircrafts just adding a modification in the tank, we have decided also to simulate a design with a single tank to reduce the wet surface and save weight in pipelines. Fig. 3.4, 3.5 and 3.6 show frontal, lateral and isometric views of the CAD design of the modified Airbus A320 aircraft with the larger hydrogen fuel tank, while Table 3.1 summarizes the dimensions of the modified fuel tank.

The way we have ended in the edges the tank has been taken arbitrarily, it can change a lot of things the design of the edges and that is another TFG itself, so we can't get into it so we followed the curvature of the actual aircraft.

The purpose of this research is not to design the most performing modified aircraft with optimum tank configuration. This would be another long, ambitious project in itself. That is why the edges and corners of the new tank, as well as how it is integrated in the modified aircraft, has not been the object of a careful study aimed at achieving best performance. Rather, the design of those features has been done arbitrarily, but trying not to change many of the design parameter of the edges and, for example, we followed the curvature of the conventional aircraft

Fig. 3.4 Frontal view of a CAD design of the modified Airbus A320 aircraft with the larger hydrogen fuel tank.

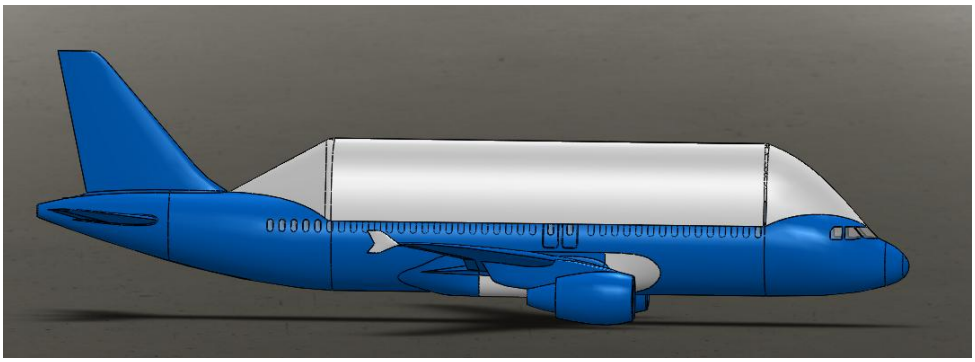

Fig. 3.5 Lateral view of a CAD design of the modified Airbus A320 aircraft with the larger hydrogen fuel tank.

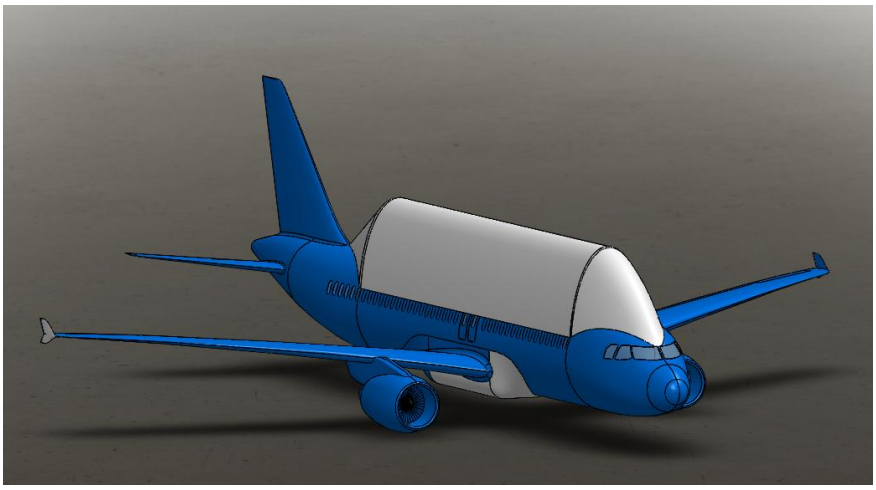

Fig. 3.6 Isometric view of a CAD design of the modified Airbus A320 aircraft with the larger hydrogen fuel tank.

Table 3.1 Dimensions of the fuel tank of the modified A320 aircraft.

FUEL TYPE	VOLUME [m^3]	HEIGHT[m]	WIDTH [m]	LENGTH [m]
HYDROGEN	120.76	2.37	3.46	18.71

3.1.2. Tanker truck fuel tank.

At present day, most of the tanker trucks are powered by diesel fuel. This is the best choice because of its high fuel efficiency and longer engine lifetime compared with gasoline engines [23].

However, combustion of diesel fuels causes significant emissions of GHG [24], and this should be prevented. Hydrogen combustion does not cause emission of GHG but hydrogen fuel occupies 4.2 times more volume than diesel fuel, for an equivalent energy, due to its lower energy density [25].

3.1.2.1. Nominal diesel fuel tanker truck.

The modified tanker truck designs that will be proposed in subsequent sections are all based in a nominal diesel fuel tanker truck, which is characterized by a maximum fuel tank capacity of 40000 L. This is a typical value of capacity that has been extracted from many truck sales and manufacturer websites. From this value, the equivalent hydrogen volume needed and modified tank dimensions will be computed.

The fuel tank of the nominal diesel fuel tanker truck is modelled as a cylinder with capacity to store 40000 L. The radius of the tank (1.03 m) is chosen to achieve an acceptable length according with the current operating tanker trucks, and thus the cylinder length can be computed as:

$$\mathrm{L} = \frac{\mathrm{V_{Diesel}}}{\pi \mathrm{r}^2} = 12\ \mathrm{m}$$

The cabin length is approximately 2.5 meters, and therefore the total length of the truck will be 14.5 m. Fig. 3.7 shows the CAD design of the nominal diesel fuel tanker truck, while Table 3.3 summarizes the dimensions of the vehicle.

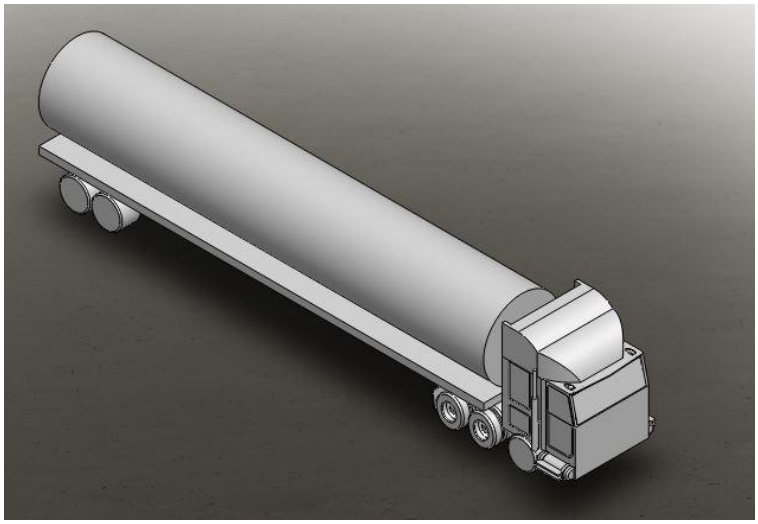

Fig. 3.7 CAD design of diesel fuel tanker truck.

3.1.2.2. Hydrogen fuel tanker truck with a single tank (rigid truck).

The modified fuel tank of the hydrogen fuel tanker truck with a single tank is also modelled as a cylinder. Taking into account that hydrogen would occupy 4.2 times more volume than diesel, for an equivalent energy, the volume of the modified hydrogen fuel tank is:

$$V_{Hydrogen} = 4.2 \cdot 40\ m^3 = 168\ m^3$$

And thus the needed length for a cylinder to store this volume is and keeping constant the radius used before is:

$$L_{r=1.03} = \frac{V_{Hydrogen}}{\pi r^2} = 50.40\ m$$

At present day, a truck with this length is not able to circulate in Spain. Therefore, there is no other way than increasing the radius in order to reduce the length of the truck.

$$L_{r=1.3} = \frac{V_{Hydrogen}}{\pi r^2} = 31.64\ m$$

We are still overcoming the maximum length allowed by the Spanish laws so we continue increasing the value of the radius.

$$L_{r=1.6} = \frac{V_{Hydrogen}}{\pi r^2} = 20.89\ m$$

As we can see, in Fig.3.8, showing the CAD design of the hydrogen fuel tanker truck with a single tank, the length of this truck is very large. Nevertheless, since the approval of mega trucks, the proposed dimensions of this vehicle (see Table 3.3) would be compliant with the Spanish laws. However, the problem of this truck consisting only of a single fuel tank is that it would feature very low manoeuvrability, movement in urban areas would be very limited and a forbidden width dimension.

Fig. 3.8 CAD design of hydrogen fuel tanker truck with a single tank (rigid truck).

3.1.2.3. Hydrogen fuel tanker truck with double tank (articulated truck).

In order to solve the manoeuvrability problem mentioned in the previous section, in this section, the large fuel tank is divided into two fuel tanks with equivalent overall volume. Therefore, the volume of one of these tanks is:

$$V_{Hydrogen/tank} = \frac{168\ m^3}{2} = 84\ m^3$$

Thus, the length of each tank must be:

$$\mathrm{L_{r=1.3}} = \frac{V_{Hydrogen/tank}}{\pi r^2} = 15{,}82\ m$$

And the total length of the truck would be:

$$L_{TOTAL} = 15{,}82 \cdot 2 + lenght\ of\ the\ cabin > 25.25\ m$$

This length is longer than 25.25 meters which is the maximum length allowed by the Spanish traffic laws [26], so this model is not feasible. Then, there is no option but to reduce the tank's fuel capacity. After making some computations shown in Table 3.2 and keeping the radius of the tank constant and equal to 1.3 m in order to be compliant with the Spanish laws, the maximum fuel capacity and length for each tank must be:

$$V_{Hydrogen/tank} = 57.4\, m^3$$

$$L = \frac{V_{Hydrogen/tank}}{\pi \cdot r^2} = 10.81\, m$$

Table 3.2 Computations done in order to obtain the maximum storing capability of the tank and being compliant with the Spanish laws.

VOLUME/TANK [m^3]	RADIUS [m]	LENGTH/TANK [m]	TRUCK LENGTH [m]
53	1.3	9.88	23.4
56	1.3	10.55	24.734
57.4	**1.3**	**10.81**	**25.25**
58	1.3	10.92	25.48
60	1.3	11.3	26.234

Now, the truck dimensions are compliant with the Spanish laws, while improving also the truck's manoeuvrability. Pitifully, we must have to reduce the total volume a 31, 66 %.

Fig.3.9. shows the final CAD design of the hydrogen fuel tanker truck with double tank, while Table 3.3 summarizes the dimensions of the vehicle.

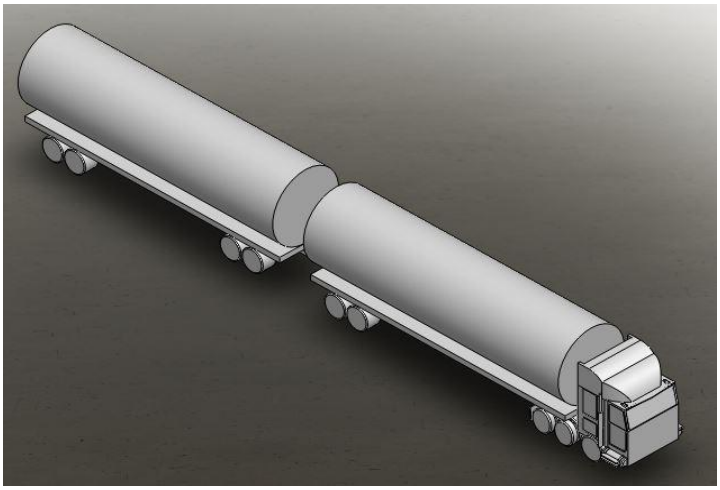

Fig. 3.9 CAD design of hydrogen fuel tanker truck with double tank (articulated truck).

Table 3.3 Overall vehicle dimensions.

FUEL TYPE	VOLUME [m^3]	Nº TANKS	HEIGHT [m]	WIDTH [m]	LENGTH [m]
DIESEL	40	1	3.06	2.060	14.43
HYDROGEN	168	1	4.12	3.2	23.32
HYDROGEN	114.8	2	3.06	2.6	25.25

3.1.2.4. Spanish laws regarding trucks.

3.1.2.4.1. Definition of truck.

By definition, a truck is a “vehicle with four or more wheels, designed and built for transporting goods, whose cockpit is not integrated with the bodywork and having a maximum capacity of nine seats, including the driver [27].”

Following construction criteria, we can say that our vehicle is a truck due to the isolated cockpit. On the other hand, and following criteria related to the use of the vehicle, we can be more specific and state that our truck is a tanker truck.

3.1.2.4.2. Maximum allowed mass and dimensions of trucks.

The European laws distinguish between two types of trucks: rigid trucks and articulated trucks.
Table 3.4 shows the maximum allowed truck dimensions stated by the Spanish laws depending on the type of truck.

Table 3.4 Maximum allowed truck dimensions stated by the Spanish laws depending on the type of truck.

RIGID TRUCK	DIMENSIONS	ARTICULATED TRUCK	DIMENSIONS
Max. Mass	31 T	Max. Mass	38 T
Max. Length	12 m	Max. Length	16.50 m
Max. Width	2.55 m	Max. Width	2.60 m
Max. Height	4 m	Max. Height	4.50 m

3.1.2.4.3. Mega trucks law.

Technological improvements have allowed better infrastructures and better vehicle designs. Therefore, circulation of mega trucks is permitted in Spain since 2016. Mega trucks are vehicles with larger dimensions and masses than the ones generally established (see Table 3.4). These kinds of vehicles improve the efficiency and security of the road transport industry, allowing the markets to be more competitive.

The *Dirección General de Tráfico* (DGT) published a new allowed truck configuration: a maximum mass of 60 T and a total length of 25.25 m for this kind of trucks. However, due to their dimensions, mega trucks are not able to circulate in all the roads as they exhibit several problems. Therefore, the route has to be programmed before and many security factors have to be taken into account.

3.1.2.4.4. Law enforcement.

In this section, the truck models proposed in this work are cross-checked against the present Spanish laws in order to see which could be the ideal truck model to comply with the law.

NOMINAL DIESEL FUEL TANKER TRUCK

This is the actual model circulating in our roads. It has been designed as an articulated model. However, it could be designed as a rigid model.
In Table 3.5, it is shown a comparison between the truck dimensions and the maximum allowed dimensions as stated by the law.

Table 3.5 Dimensions of nominal diesel fuel tanker truck cross-checked against the present Spanish laws.

DIMENSION PARAMETER	NOMINAL DIESEL TRUCK DIMENSIONS	LAW DIMENSIONS	ACCOMPLISHMENT
Max Length	14,43 m	16,50 m	YES
Max Width	2,06 m	2,60 m	YES
Max Height	3,07 m	4,50 m	YES

HYDROGEN FUEL TANKER TRUCK WITH A SINGLE TANK (RIGID TRUCK)

In previous sections, we have seen that hydrogen is a gas that occupies more volume than diesel. Thus, when having the truck powered by hydrogen, the tank needed to store the same quantity of fuel as in the diesel case, is much bigger.

We have tried that hydrogen tank dimensions were suitable with the Spanish laws, so, with the target to store the same quantity of fuel, the tank could have a larger length reducing the diameter of the tank or instead of increasing the length of the tank, we could reduce the length and increase the diameter until both dimensions were compliant with the law.

Pitifully it has been seen that is impossible to build a truck with a single hydrogen tank that respects the Spanish laws. We conclude that at present day, and with the current technology, it is impossible to obtain a hydrogen fuel tanker truck with a single tank able to circulate in the current Spanish roads.

Table 3.6 shows a comparison between the truck dimensions and the maximum allowed dimensions stated by the law.

Table 3.6 Dimensions of hydrogen fuel tank tanker truck with a single tank (rigid truck) cross-checked against the present Spanish laws.

DIMENSION PARAMETER	ONE HYDROGEN TRUCK DIMENSIONS	LAW DIMENSIONS	ACCOMPLISHMENT
Max Length	23.32	25.25	YES
Max Width	3.20	2.60	NO
Max Height	4.12	4.50	YES

HYDROGEN FUEL TANKER TRUCK WITH DOUBLE TANK (ARTICULATED TRUCK)

It is important to recall that this model does not have the same volume capacity: it was reduce to be able to comply with the law. However, we attempted tries to obtain the maximum possible volume capacity. Table 3.7 shows a comparison between the truck dimensions and the maximum allowed dimensions as stated by the law.

Table 3.7 Dimensions of hydrogen fuel tanker truck with double tank (articulated truck) cross-checked against the present Spanish laws.

DIMENSION PARAMETER	DOUBLE HYDROGEN TANKER TRUCK DIMENSIONS	LAW DIMENSIONS	ACCOMPLISHMENT
Max Length	25.25 m	25.25 m	YES
Max Width	2.60 m	2.60 m	YES
Max Height	3.048 m	4.50 m	YES

3.1.3. Control volume definition.

In previous sections we have seen the new design of the aircraft and tanker truck including the hydrogen tank. Once the geometry has been designed, we have to define the control volume using the enclosure tool.

By selecting this tool, we create an enclosure surrounding our solid, such that we have two domains (enclosure and solid), but we need only one: the fluid domain that will be the control volume. The Boolean tool allows us to subtract the aircraft body from the enclosure, leaving a single domain (see Fig. 3.10). The size of the control volume is very important because it can affect the results of the simulation. Thus, we will discuss now the size of this control volume.

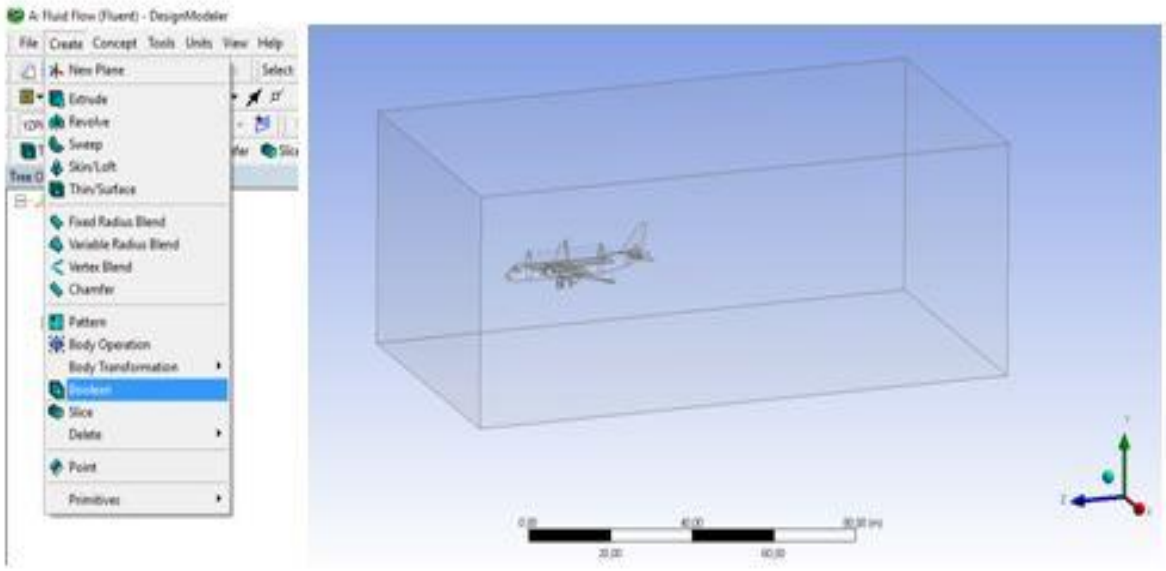

Fig. 3.10 Boolean tool in ANSYS-Fluent.

As said before, the size of the control volume may affect the final results of the simulation, namely, the aerodynamic performances of the vehicles. It is thus necessary to make what is called a control volume independence study; that is, to study when the obtained results become independent of the size of the control volume. The control volume size in the z axis is the most important affecting the drag coefficient (see reference frame in Fig. 3.10), so the study has been done keeping the other dimensions constant (see Tables 3.8 and 3.9).

Table 3.8 Control volume dimensions.

AXIS	DISTANCE FROM AIRCRAFT [m]
X	20
Y	20
Z	20
-X	20
-Y	20
-Z	20, 40, 60, 80, 90, 100 and 105

Table 3.9 Drag coefficient obtained for the different control volume dimensions.

DISTANCE FROM AICRAFT (-Z) [m]	C_D
20	0.0415834
40	0.0425645
60	0.0439502
80	**0.0505980**
90	0.0471271
100	0.0479416
105	0.0485203

The problem is that increasing the size of the control volume causes an exponential increase of the number of cells inside the mesh, so it takes longer time for the simulation to converge. Thus, a compromise is necessary between the computational cost (simulation time) and the desired independence from control volume size and accuracy. We decided to work with a distance of 80 m because of the similarity between the results obtained from the 80 m simulation. The results vary a little bit in every simulation you do but, the variation between 80 m, 90 m, 100 m, and 105 m is so small. As we said every simulation increasing the size of the control volume increases the simulation time, so choosing the 80 m is the best option due to the little variation that appears in the subsequent drag coefficients that would suppose an unnecessary extra simulation time.

3.2. Mesh.

Meshing is one of the most important steps of CFD analysis, where the size of the control volume and the quantity of cells in the mesh relate to each other. At present day, meshing may not be as difficult as it was before, but the automatic mesh that ANSYS generates may not be suitable for particular simulations. In these cases, different features can be chosen (see Fig. 3.11).

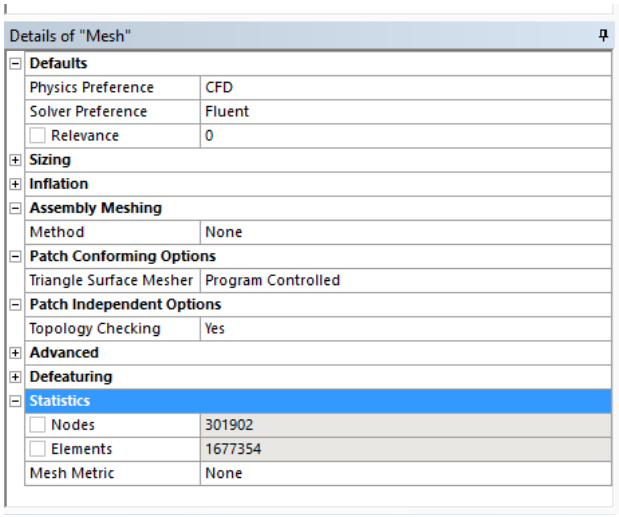

Fig. 3.11 Mesh options in ANSYS-Fluent.

Fig. 3.13 and 3.14 show the meshes for the fluid problems corresponding to the A320 aircraft modified to account for the new hydrogen tank, and the tanker truck, respectively.
For example, in the first case there are 1.677.354 cells. It can be a small number of cells but the important thing is their size and growth rate like in Fig. 3 12. By controlling the minimum size we can assure that in complex geometries the solution will be accurate. The *growth rate* tool allows us to be able to control the solution in each cell, this way, avoiding large/abrupt changes between the computed solutions in the previous and surrounding cells. With the size cell independence study we did, the best option for us is the *Proximity and*

curvature with *coarse Relevance center*. When *relevance center* is defined as fine, it gives more accuracy but the amount of computational cost does not worth the small gain we obtain.

Relevance	0
Sizing	
Use Advanced Size Function	On: Proximity and Curvature
Relevance Center	Coarse
Initial Size Seed	Active Assembly
Smoothing	Medium
Transition	Slow
Span Angle Center	Fine
Curvature Normal Angle	Default (18,0 °)
Num Cells Across Gap	Default (3)
Min Size	Default (8,1879e-002 m)
Proximity Min Size	Default (8,1879e-002 m)
Max Face Size	Default (8,18790 m)
Max Size	Default (16,3760 m)
Growth Rate	Default (1,20)
Minimum Edge Length	1,5462e-004 m
Inflation	
Use Automatic Inflation	None
Inflation Option	Smooth Transition

Fig. 3.12 Mesh cells settings for sizing and growth.

This relates intimately to the size of the mesh cells and the desired quality of the mesh. The size of the cells surrounding the vehicles (typically the smallest cells) is critical; it depends on the desired resolution of the results, the smallest surfaces, entities and relevant features in the CAD geometry of the vehicles, etc. The size of the cells reaching the surfaces limiting the control volume (typically the largest cells) is chosen such that the computation times are reasonable. The quality is chosen in the sizing selection. For our simulations we chose to enable the sizing in the *Proximity and curvature* mode.

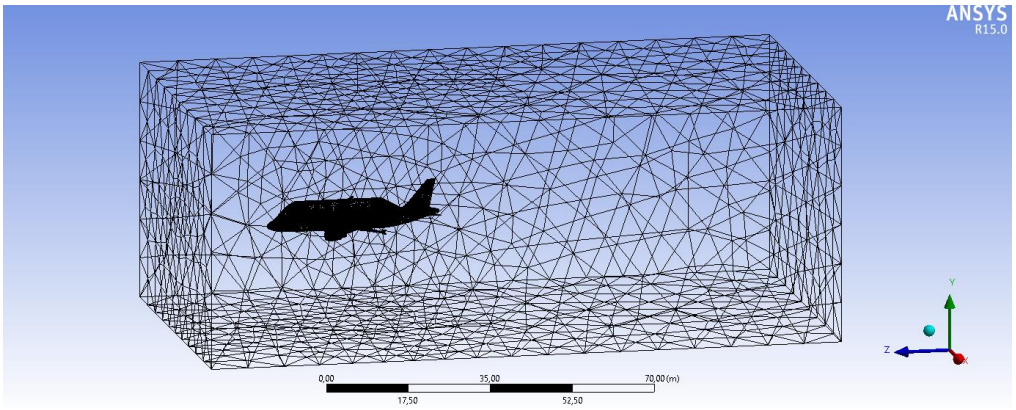

Fig. 3.13 Mesh for the fluid problem of the A320 with hydrogen tank.

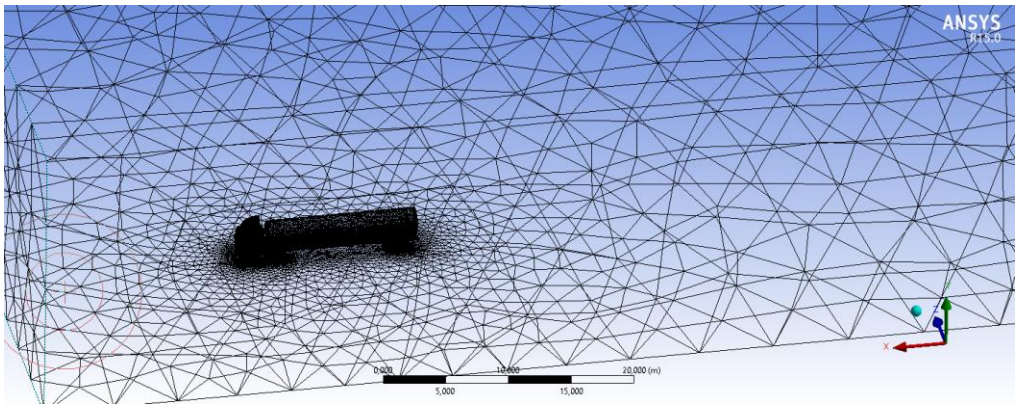

Fig. 3.14 Mesh for the fluid problem of the tanker truck.

3.2.1. Mesh quality check.

If the mesh is created correctly, it would appear in black colour, but, if it is not the case, there are some factors to be taken into account (before moving on to the next step of the CFD analysis). The Fig. 3.11 shows the *Mesh Metric* tool, which gives some indicators about the quality of the mesh. A good quality of the mesh is usually associated with a better convergence to the solution. Otherwise, the simulation may not converge to the solution.

There are two important indicators to measure the quality of the mesh:

- **SKEWNESS**

The tolerance of the points in the mesh is shown in Fig. 3.15. Comparing the results of the Skewness on our simulation (see Fig. 3.16); we can see that all points are in the recommended range.

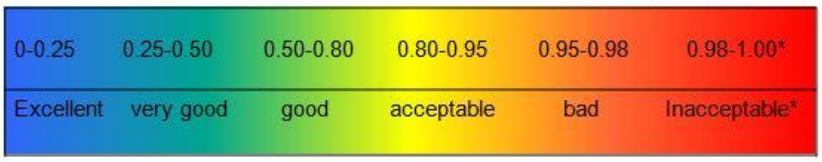

Fig. 3.15 Mesh quality depending on the skewness values.

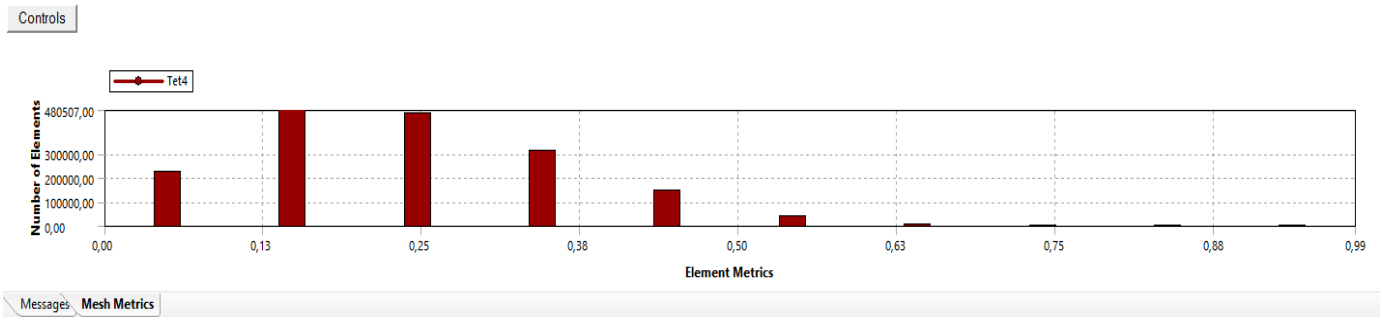

Fig. 3.16 Skewness values obtained for the A320 mesh simulation.

- **ASPECT RATIO**

The aspect ratio of the geometry can be defined as the relation between its width and its height. It can be computed as the ratio between the longest edge and the shortest edge. It has to be below 40, but in the cells of maximum inflation it can be tolerated higher than 50.

Comparing the aspect ratio of our mesh the range described above, we can see that, for most of our cells, the aspect ratio ranges between 1.16 and 44.51 (see Fig. 3.17 and 3.18). Although all the cells are in the recommended range, the quality of our mesh could be improved, but the marginal enhancement in accuracy of the solution that we would obtain is not worth enough in relation to the associated increase in computational load. In view that both skewness and aspect ratio values are in the acceptable ranges, it is most likely that our simulation is going to converge into a solution.

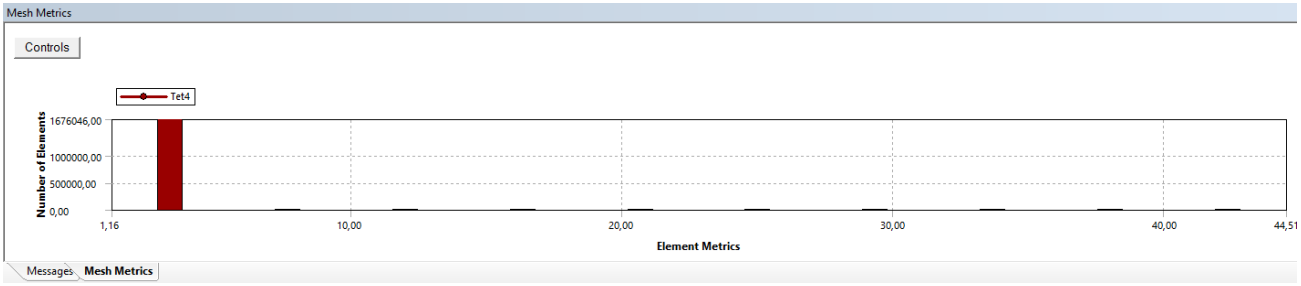

Fig. 3.17 Aspect ratio values obtained for the A320 mesh simulation.

Statistics	
Nodes	301902
Elements	1677354
Mesh Metric	Aspect Ratio
Min	1,1639
Max	44,51
Average	1,86793944426759
Standard Deviation	0,511031875334491

Fig. 3.18 Minimum, maximum and average values of aspect ratio.

3.3. Definition of the boundary conditions and the physics of the problem.

Before moving on the next step of the CFD analysis, we have to define some settings. The settings affect, for example, all the surfaces of our control volume (fluid domain), in which we must define some restrictions.

In CFD, we can usually distinguish between four kinds of boundary conditions:

- **WALL**

The walls are boundaries in which the air flow either fulfils the no-slip condition (if the fluid has viscosity) or has velocity tangential to the surface (if the fluid I assumed ideal). If the walls are sufficiently far away from the vehicle, they do

not affect the results of the simulations (that is the purpose of the control volume independence study). They have to be used because we cannot simulate an infinite control volume. Also, they do not affect anything in the flow such as the inlet and the outlet surfaces.

- **OUTLET**

The outlets (for example, the backward surface, usually) are those boundaries through which we expect the flow to abandon our control volume (see Fig. 3.19). We often define the pressure of the flow abandoning our control volume through that surface, in what is called a “pressure outlet” boundary condition.

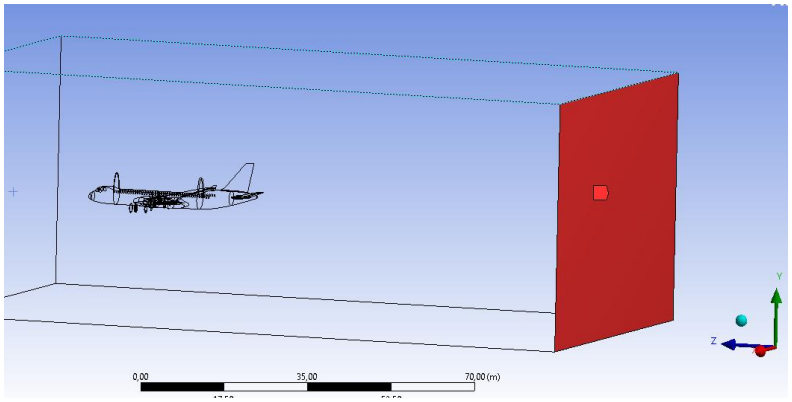

Fig. 3.19 Outlet surface for our control volume in the modified A320 simulations.

- **INLET**

The inlets are those boundaries through the flow enters into our control volume. They are among the most important surfaces of the control volume (see Fig. 3.20). As for the ·”pressure outlet”, we can define the pressure of the flow entering our control volume, but it is often more convenient to define the speed of the entering flow as well as its orientation, in what is called a “velocity inlet” boundary condition. This, combined with “pressure outlet”, is a recommended pair of boundary conditions in many fluid problems.

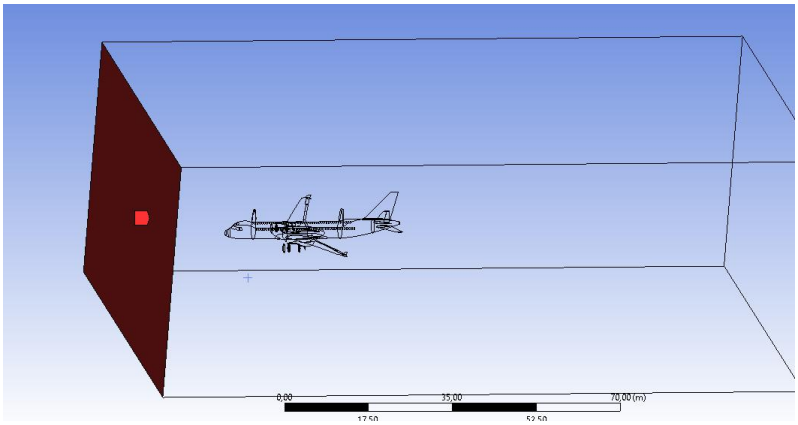

Fig. 3.20 Inlet surface for our control volume in the modified A320 simulations.

- **BODY SURFACE**

As important as the inlet is the body surface, the contact area between our vehicle and the fluid. Careful definition of this type of surfaces is necessary for being able to compute, for instance, the lift and drag coefficients.

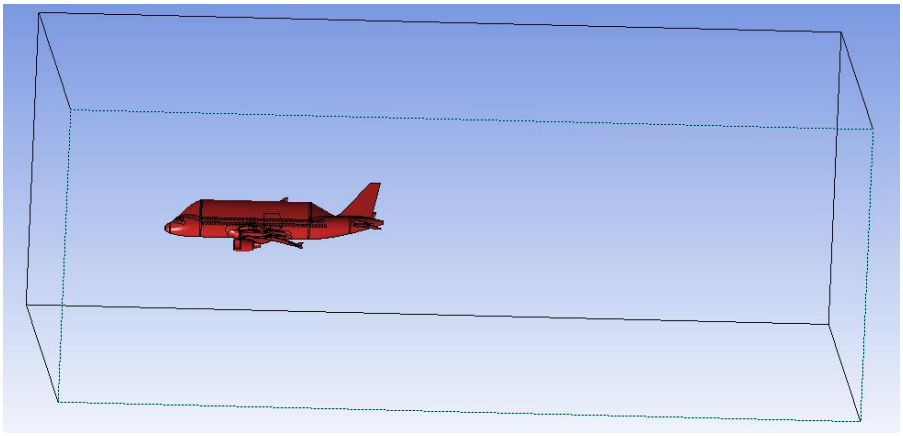

Fig. 3.21 Body surface for the modified A320.

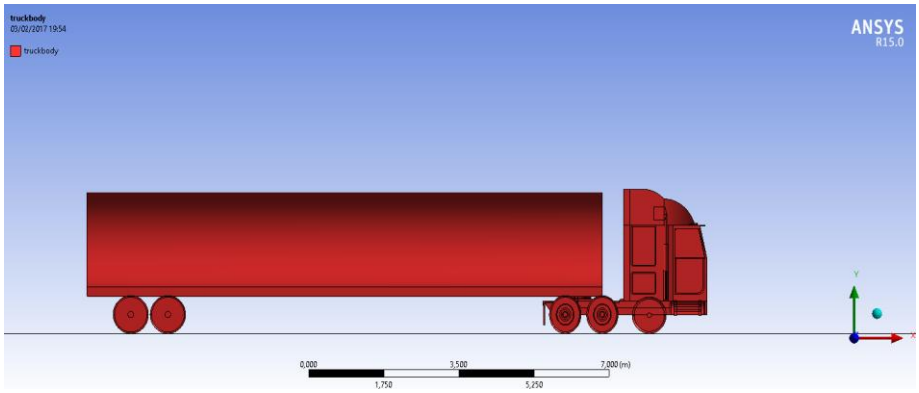

Fig. 3.22 Body surface for the tanker truck.

3.4. Setup.

The setup step allows us to establish some settings when performing the computation. These settings are defined, for instance, whether the processing is serial or parallel depending on our processing configuration. It also allows changing the display options.

3.5. Solution

Most of the settings to make the simulations as similar as possible to the reality are chosen in this step. Next, we will explain in detail the settings we used in our simulations.

GENERAL

These settings allow establishing the configuration for the solver. The velocity formulation, type of solution based on pressure and density and the time configuration steady or transient (as shown in the Fig. 3.23). It is important to highlight that our problem is steady, so no fluid property will depend on time.

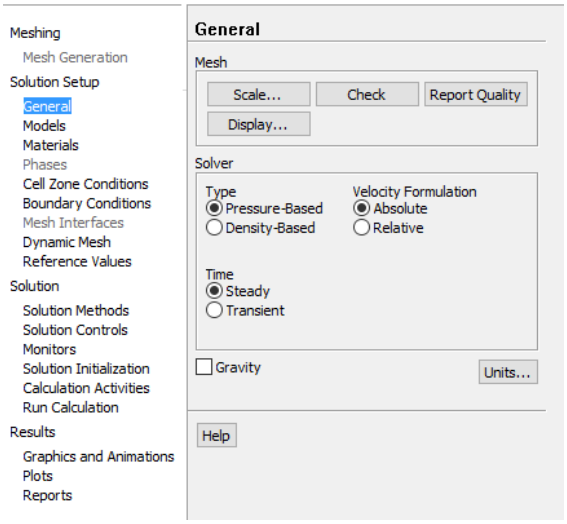

Fig. 3.23 *Solution* setup.

MODELS

In previous sections we saw that the aircraft and tanker truck problem are high Reynolds number scenarios. Hence, the airflow will be turbulent.

In our simulations, we used the k-epsilon turbulence model, which is the most common model used in CFD to simulate mean flow characteristics for turbulent flow conditions. The variable k is a measure of the energy in the turbulence flow, and is called turbulent kinetic energy. The variable ξ is the turbulent dissipation which determines the rate of dissipation of the turbulent kinetic energy.

MATERIALS

The properties of the simulated fluid inside the control volume (in our case air) can be edited (e.g., density and viscosity).

CELL ZONE CONDITIONS

In this step, it is only necessary to change condition of the domain enclosed by the control volume, from Solid to Fluid. This way, in the next steps it will be easier to understand what is being addressed, and thus, avoid mistakes.

BOUNDARY CONDITIONS

This part is one of the most important because it allows us to set the values of the magnitudes, such as the velocity, that will affect the model. Thus, here is when defining the physics and real conditions of the problem. For example, in the inlet surface, a value of 230 m/s is settled for the incoming velocity of the flow in the aircraft study, and a value of 22.22 m/s in the tanker truck study.

NORMAL OR DYNAMIC MESH

Normal meshes are constructed on geometries which are physically not going to change. For most CFD simulations the physical geometry does not change with time, and a steady mesh will be the appropriate choice. On the contrary, dynamic meshing refers to situations in which the computational grid changes during the execution of the simulation. For example, dynamic meshes allows simulating flows where the geometry changes with time, e.g. flows around falling objects, etc. Therefore, our study is carried out using a normal mesh.

REFERENCE VALUES

In this step, there are a few things to take into account. We have to select Compute from inlet in Reference Zone fluid. The data we must change to obtain good results are the *Area* and *Temperature*. These values will be used in computing, for instance, the aerodynamic coefficients (that is, the lift and drag coefficients), the main results of this study. All the other data was changed in previous steps.

The *Area* is the frontal area of our vehicles. To compute this area we have to select *Reports* (see Fig. 3.24). Inside *Reports* we have to select *Projected Areas*, and select the body surfaces we defined before, the axis along which our flow is moving and click compute.

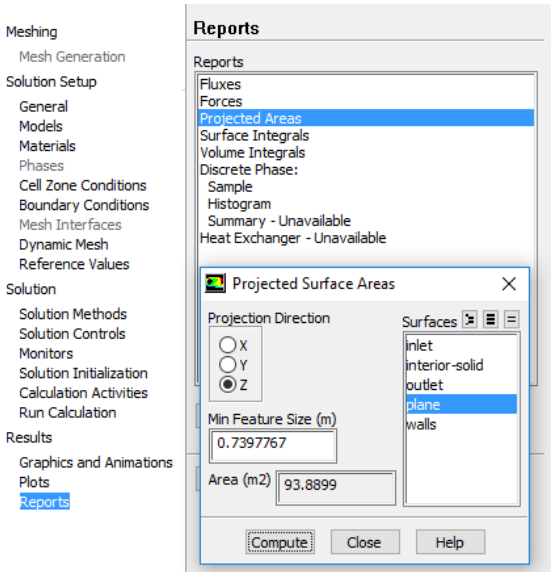

Fig. 3.24 *Frontal Area* computation.

SOLUTION METHODS

There are many different methods to solve fluid problems. The one we have chosen is the coupled method. It involves higher computational load than the simple method but it is more accurate because it couples the calculation of the pressure and velocity fields.

SOLUTION CONTROLS

Once the method is selected, we can also define additional settings to make the simulation even more accurate.

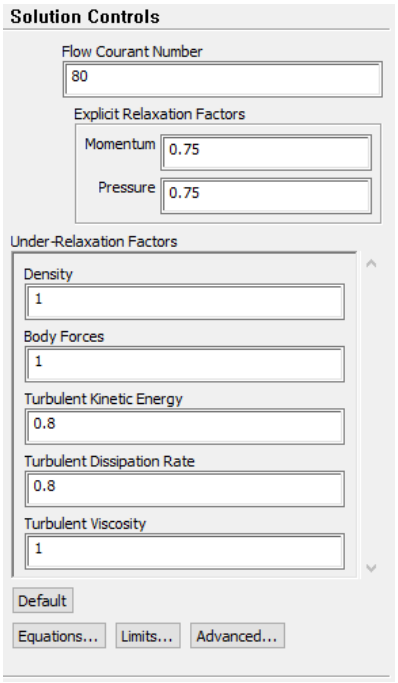

Fig. 3.25 *Method options*.

MONITORS

In *Monitors* is where we select the parameters that we want to monitor during the simulation. These data can be displayed graphically during the simulation and also in a txt file. To achieve this, we selected *Create a new Force Monitor,* then we selected the kind of monitor, (C_D and C_L in our case).

SOLUTION INITIALIZATION

This step is important to reset the initial values in case we want to change them. To do so, it is simply necessary to change the values select *Standard initialization, Compute from Inlet and Initialize.*

CALCULATION ACTIVITIES

The *Auto- save* every (iterations) tool allows saving the iterations done (and results obtained) when simulating, to have some results saved in intermediate

stages of the simulation process as a back-up. Therefore, if there is a power outage, the process has been saved at a certain number of iterations.

RUN CALCULATION

Here we define the number of iterations to be computed. This has a computational cost, that is, if we add more iterations the simulation will usually take more time to be completed. However, if we set more iterations the results are more accurate. For example, we chose twenty iterations since normally the results in our simulations have converged after these twenty iterations and the accuracy improvements in the subsequent results are negligible and they suppose a waste of time.

To conclude this section, Table 3.10 shows a summary of the settings used for the CFD simulations. We can see that is divided in two sections, the solver and the reference values which allow us to have a global view of the fluid domain.

First of all, we will talk about the solver section. As we said before, the turbulence model chosen is the k-ξ method, widely used in the CFD analysis field. Momentum, Turbulent kinetic energy and momentum thickness discretization are solved by means of a second order upwind method. We chose it in order to obtain more accurate results although taking more time to converge. Least Squares Cell Based method has been chosen for the gradient discretization. In this method the solution is assumed to vary linearly. When a flow solution is solved on polyhedral meshes the cell-based least squares gradients are recommended to obtain a more accurate flow solution. However, as we have a tetrahedral mesh it would be comparable to use the node-based gradient method [28]. The PRESTO! (PREssure STaggering Option) scheme is available for all meshes.

As we said before, the reference values are those which characterize the fluid problem. The table shows the frontal area computed as said and explained in previous sections. We can see that the density is different depending on the study because the vehicle in case is moving in different altitudes and therefore due to the temperature varies. Finally, the dynamic viscosity is shown for each vehicle study and can be computed from the kinematic viscosity (see Reynolds number computations in section 2.1.2) times the density.

Table 3.10 Summary of the settings used for the CFD simulations.

SOLVER	Turbulence model	k-ξ (2 eqn)
	Pressure-velocity coupling	Coupled
	Gradient discretization	Least Squares Cell Based
	Pressure discretization	PRESTO!
	Momentum discretization	Second Order Upwind
	Turbulent kinetic energy discretization	Second Order Upwind
	Momentum thickness Re discretization	Second Order Upwind
REFERENCE VALUES	Area [m^2]	89.47 - 93.89 - 8.22 - 12.83 - 9.48[2]
	Density [kg/m^3]	Aircraft (11km):0.364 Truck (SL): 1.225
	Gauge pressure [Pa]	0
	Velocity [m/s]	Aircraft (cruise): 230 Truck: 22.22
	Viscosity [kg/m·s]	Aircraft (11 km):$1.42x10^{-5}$ Truck (SL): $1.85x10^{-5}$

[2] These values are classified depending on the frontal area as follows: Conventional A320, A320 with hydrogen fuel tank, diesel tanker truck, one single hydrogen tank tanker truck and double hydrogen tank tanker truck.

CHAPTER 4. CFD RESULTS

4.1. Graphical results.

This section shows graphical displays of the results of the simulations which allow interpreting and analyzing the behaviour of the fluid.

4.1.1. Aircraft.

The aim of the simulations was to see the different behaviour of the fluid and thus the different aerodynamic performances of the vehicles with and without hydrogen tank. By creating visualization planes perpendicular to the x axis, we can see graphically the effect of the tank by means of pressure and velocity contour plots.

To clearly observe the differences in the pressure contour plots corresponding to the simulations with and without hydrogen tank, we have to define the same range of pressures for the scales and the same amount of contours. The upper and lower limits of pressure in the colour scales to avoid losing any information depend on the results of the simulations with and without hydrogen tank. The upper and lower limits will be the maximum and minimum pressures considering both simulations.

The results shown in Fig. 4.1 to 4.8 (corresponding to pressure contour plots in the planes x = 0, x = 4.5 and x = 8 m) are in reality the differences between the pressure and the atmospheric pressure in the studied fluid domain. That is why negative values can be observed.

The settings finally selected for Fig. 4.1 and 4.2, shown in Table 4.1, were only used for the pressure contour plots in the planes perpendicular to the *x* axis. In the aircraft contours we used another configuration that will be defined later on.

Table 4.1 Settings for defining the pressure contour plots in Fig. 4.1 and 4.2.

PRESSURE	Maximum [Pa]	9968
	Minimum [Pa]	-25704
CONTOURS	Nº of contours	100

In the studied fluid domain, we have a maximum and minimum pressure. The gap between both of them is so large and they occur in such small localized regions, that we cannot observe really well variations in the fluid behaviour or appreciate the pressure contours in the rest of the fluid domain, for which the vehicle causes small or no perturbation in the incident flow and thus the pressure is very similar to the atmospheric pressure (see Fig. 4.1 and 4.2

- **Section plane: $x = 0\ m$.**

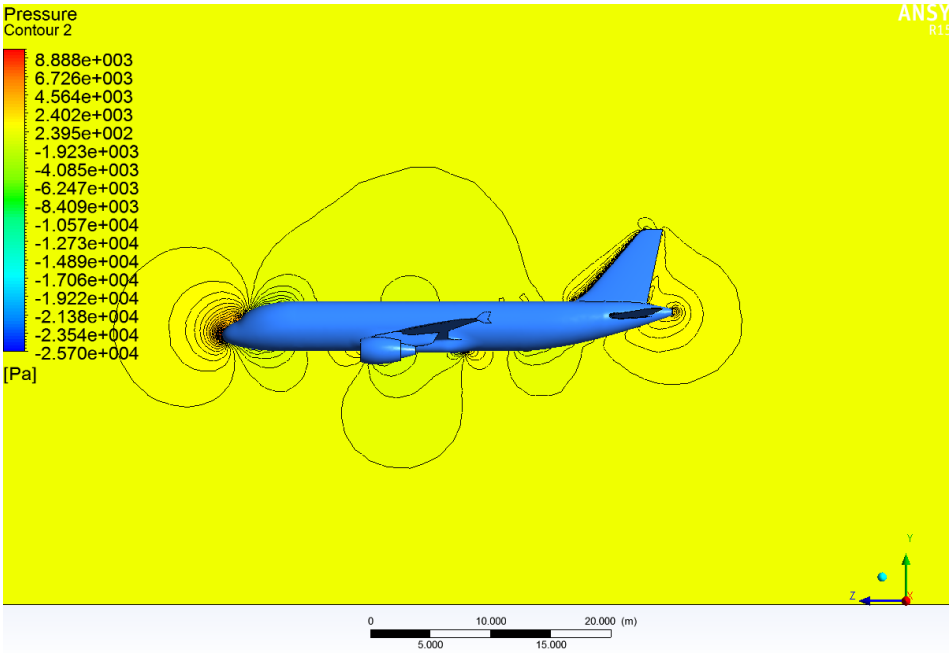

Fig. 4.1 Pressure contours for conventional A320 aircraft in plane x=0 m.

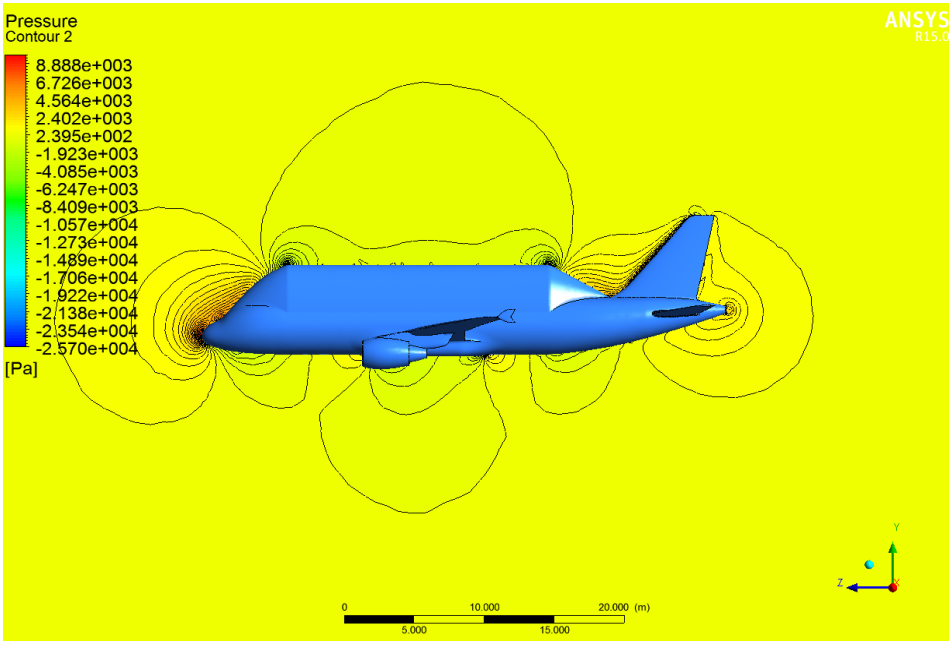

Fig. 4.2 Pressure contours for modified A320 aircraft in plane x=0 m.

To be able to appreciate better the differences, we make a zoom; bring closer the upper and lower limits of pressure in the scale. This way, we lose some information about the maximum and the minimum but we obtain more information of the other zones. The new pressure limits are defined in Table 4.2.

Table 4.2 Settings for defining the pressure contour plots in Fig. 4.3 and 4.4.

PRESSURE	Maximum [Pa]	2000
	Minimum [Pa]	-3000
CONTOURS	Nº of contours	100

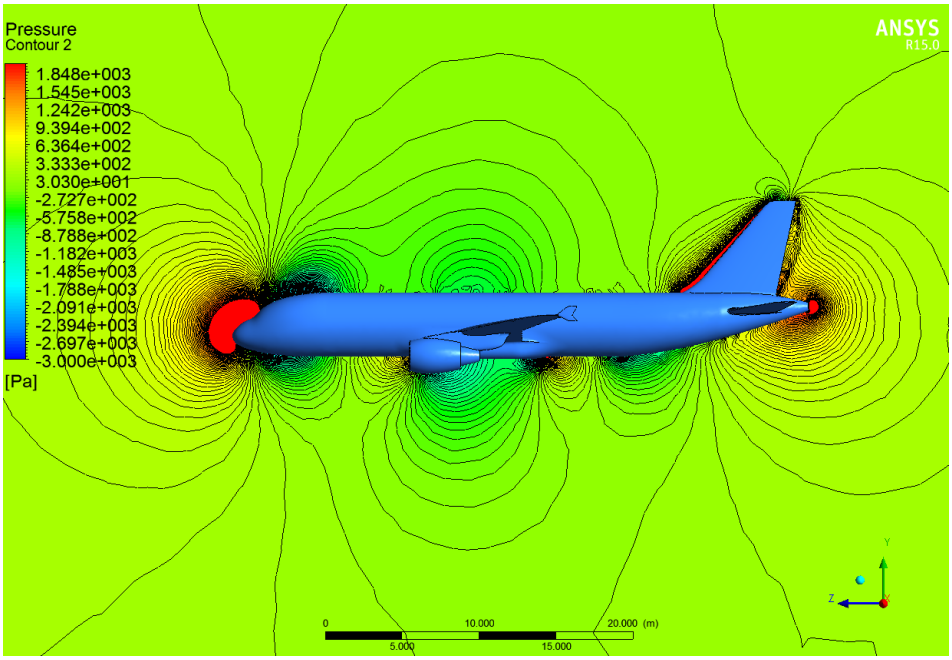

Fig. 4.3 Pressure contours for conventional A320 aircraft in plane x=0 m (zoom).

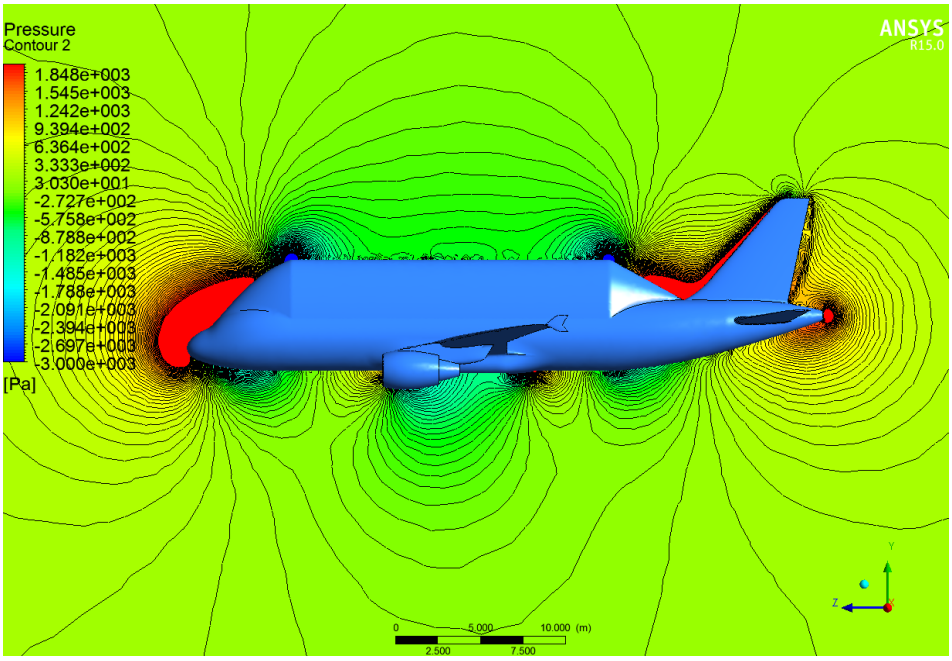

Fig. 4.4 Pressure contours for modified A320 aircraft in plane x=0 m (zoom).

Comparing Fig. 4.3 and Fig. 4.4, we can see that in both figures exists a large value of pressure in the nose of the aircraft. However, due to the existence of the hydrogen tank in the modified aircraft, the area of higher pressures is even larger as expected and stated by the Bernoulli's equation [29]. Focusing on the modified A320, the pressure is reduced when the speed is increased in the corners of the hydrogen tank. At the end of the fuel tank, the flow is abruptly detached from the surface. Because of this detachment, a large turbulent wake will be created, thus generating a pressure difference causing even more drag than in the conventional A320. Finally, in the aircrafts belly it can be appreciated that there is a small decrease on the pressure values. We think that is due to the presence of the fuel tank. When the flow clashes with the nose of the aircraft, a component of the speed flow is deviated to the belly of the aircraft and thus generating an unexpected increase of the total velocity and consequently, pressure decreases.

- **Section plane:** $\boldsymbol{x = 4.5\ m}$

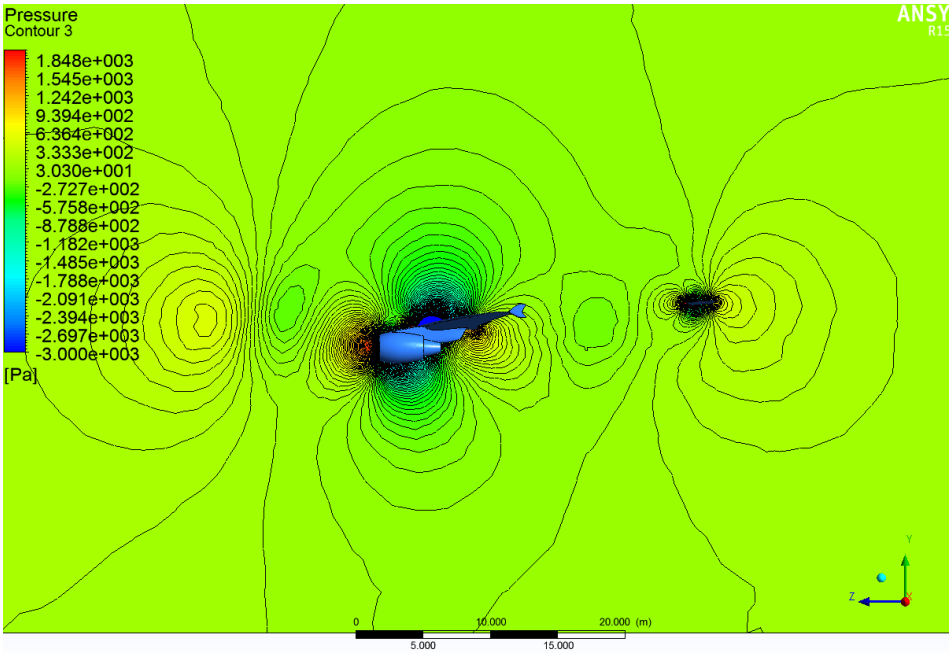

Fig.4.5 Pressure contours for conventional A320 aircraft in plane x=4.5 m.

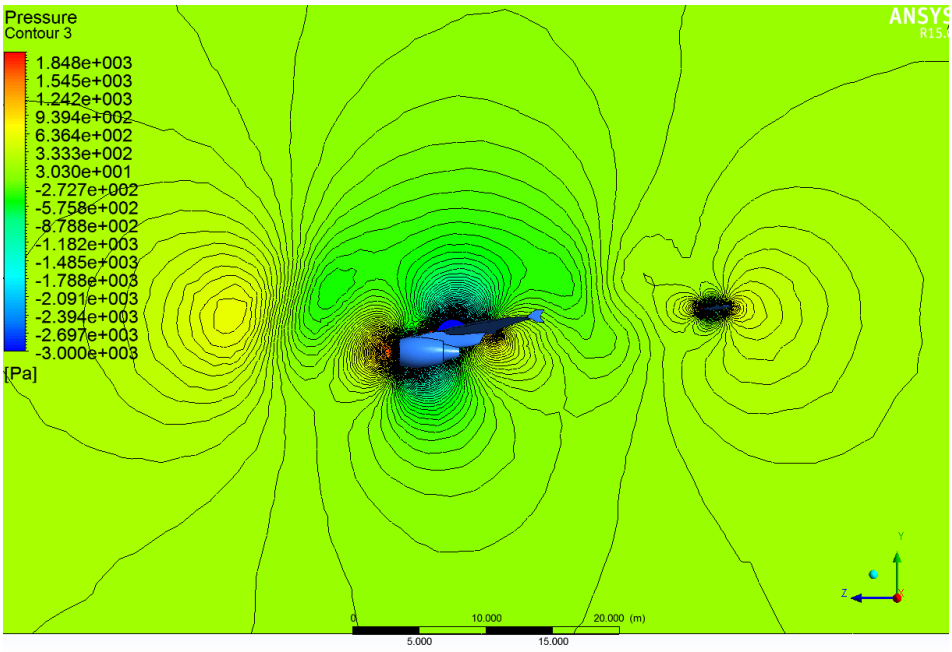

Fig.4.6 Pressure contours for modified A320 aircraft in plane x=4.5 m.

Comparing Fig. 4.5 and Fig. 4.6, we can see that both figures are very similar in the engine area. However, the pressure isobars above the engine are different because of the existence of the hydrogen fuel tank. The tank produces a deformation on them creating a larger area of lower pressures. Therefore, the speed flow along the tank is greater than if there was no tank.

- **Section plane:** $\boldsymbol{x = 8\ m}$

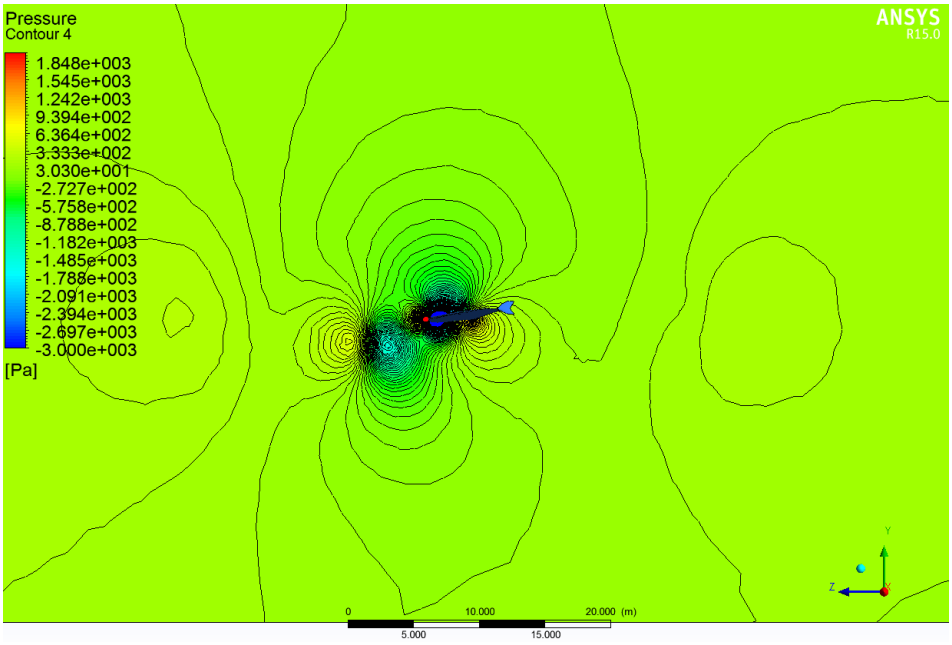

Fig.4.7 Pressure contours for conventional A320 aircraft in plane x=8 m.

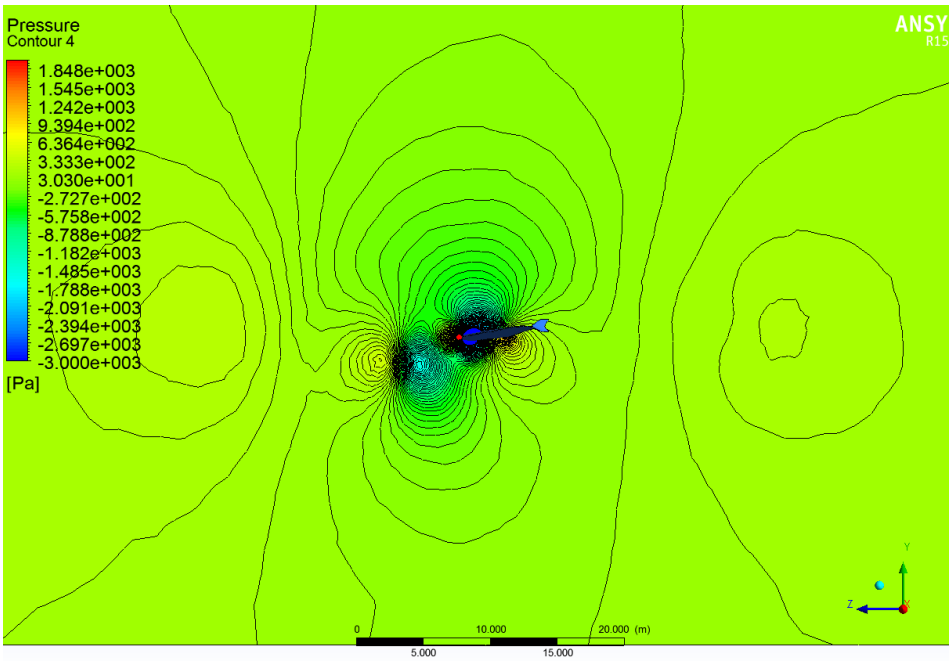

Fig.4.8 Pressure contours for modified A320 aircraft in plane x=8 m.

Comparing Fig. 4.7 and Fig. 4.8, we can see that there are not significant differences between them. Only the sizes of some isobars have changed. Hence, if we move from the hydrogen fuel tank until the wingtip, the effects caused by the hydrogen fuel tank decrease.

The contours shown so far are pressure contours but we can also observe the behaviour of the fluid velocity in the studied fluid domain by means of plots of the streamlines, velocity contours, etc. The settings chosen for visualizing the velocity contour plots are shown in Table 4.3.

Table 4.3 Settings for defining the velocity contour plots in Fig. 4.9 and 4.10.

VELOCITY	Maximum [m/s]	280
	Minimum [m/s]	0
	Nº of contours	100

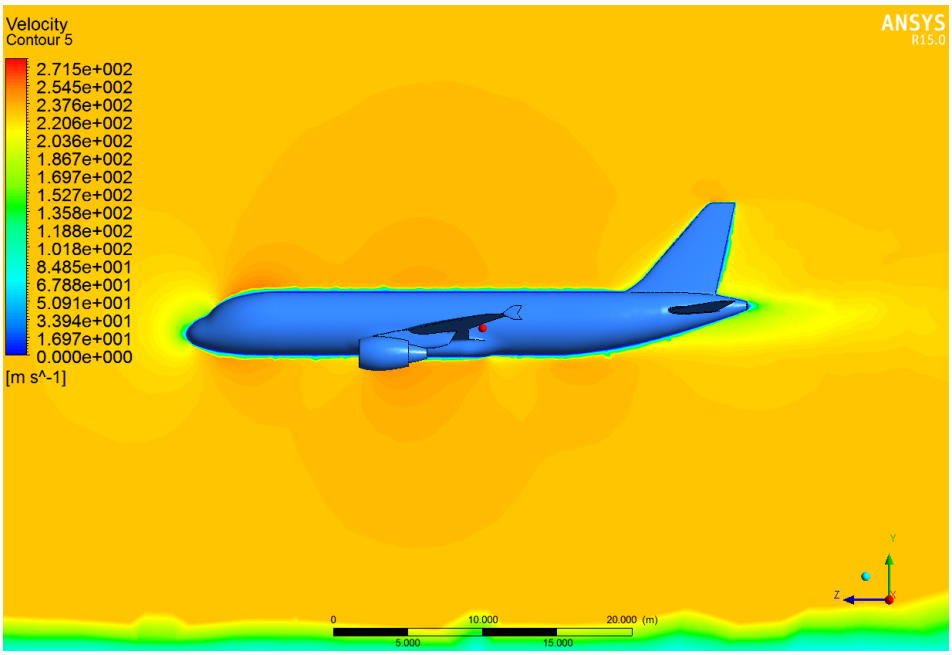

Fig.4.9 Velocity contour plot for the conventional A320 aircraft in plane x=0 m.

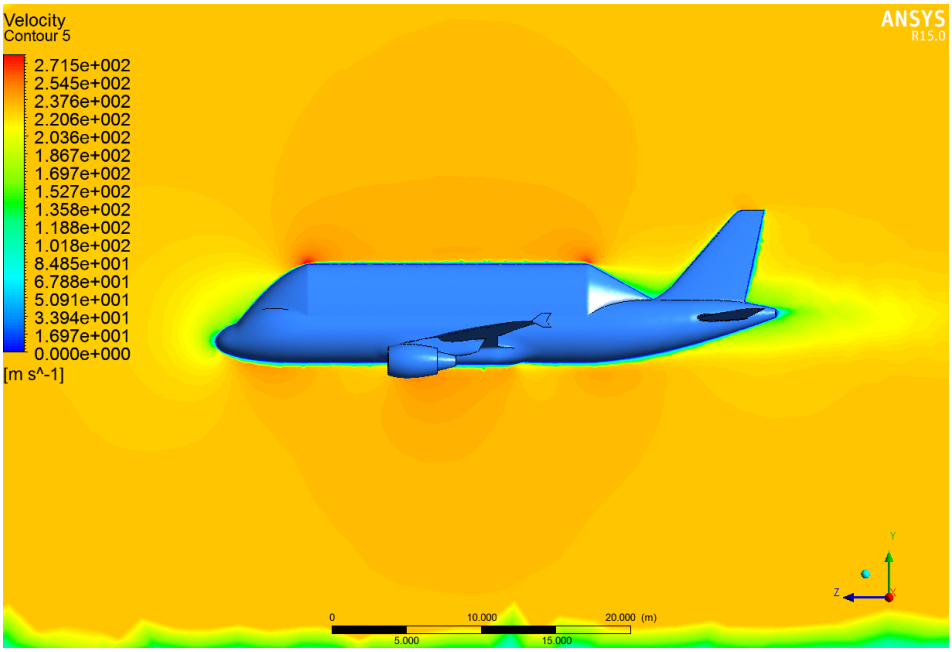

Fig.4.10 Velocity contour plot for the modified A320 aircraft in plane x=0 m.

The conservation of energy in fluid mechanics (Bernoulli's equation) states that if the velocity increases the pressure decreases and the other way around. Looking at Fig.4.9 and Fig. 4.19, the explanation we did for the Fig. 4.3 and Fig. 4.4 matches up.

Table 4.4 Aircrafts contours pressure definition.

PRESSURE	Maximum [Pa]	9968
	Minimum [Pa]	-25704
CONTOURS	Nº of contours	30

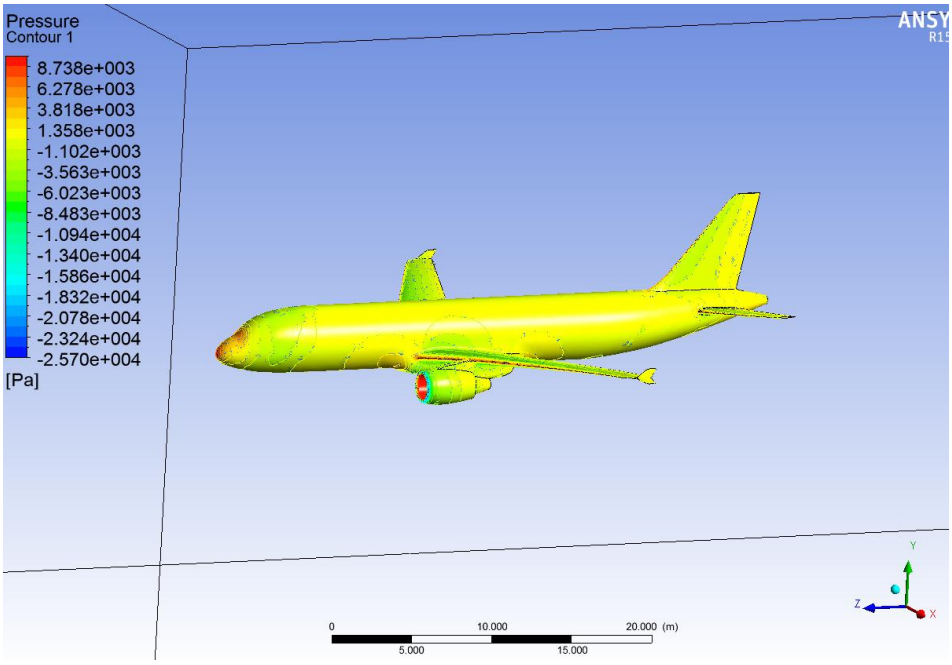

Fig.4.11 Isometric view of conventional A320 aircraft with surface pressure contours.

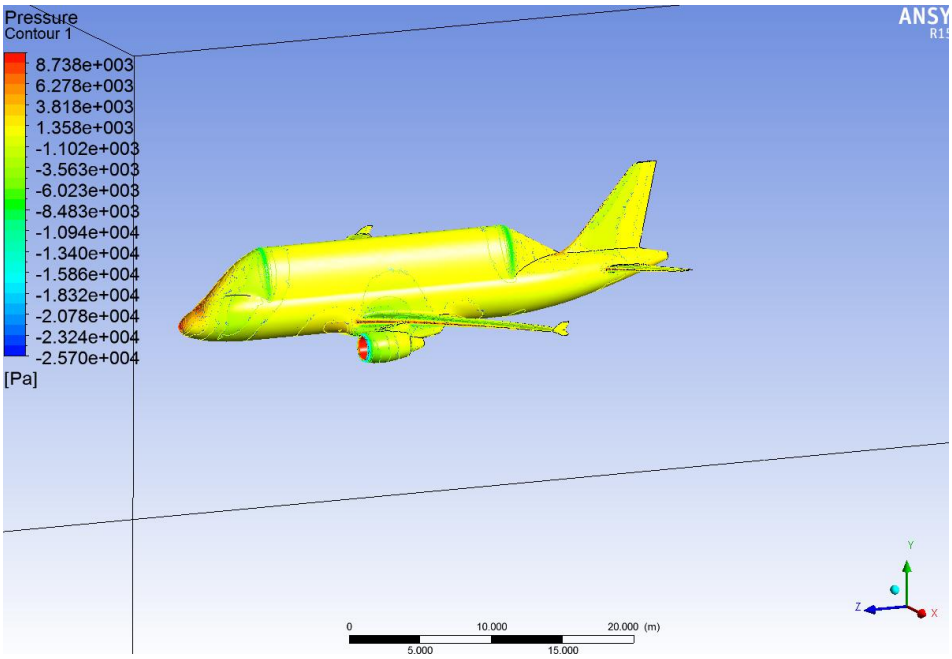

Fig.4.12 Isometric view of modified A320 aircraft with surface pressure contours.

In the aircraft, the fluid appears to behave similarly on both aircrafts. Once the fluid starts moving around the tank, differences can be observed: the pressure in the frontal area of the hydrogen tank increases. On the edge of the hydrogen tank, the pressure diminishes as expected, and, when reaching the end of the tank, the vertical stabilizer receives a turbulent higher pressure flow.

4.1.2. Tanker truck.

Fig. 4.13, 4.14 and 4.15 show the pressure contours in plane x=0 m for a conventional diesel tanker truck, and hydrogen fuel tanker trucks with a single tank and double tank, respectively. Comparing the results in these three cases, we can observe that the pressure contours in the vicinity of the cabin of the trucks are similar. As expected, the differences in the behavior of the fluid around the trucks appear around the tanks. For the diesel tanker truck, the tank is as high as the cabin so there is not extra perturbation in the fluid there.

On the contrary, the tank for the hydrogen fuel tanker truck with a single tank is higher than the cabin, so the pressure is higher in that region (the frontal part of the tank exceeding the height of the cabin) because there is some sort of stagnation. The tank for the hydrogen fuel tanker truck with double tank is a little higher than the diesel tank, but not much, so it also creates a region of high pressures, there, but not as significant. Another important issue is also the types of drag, these features are contributing to create, which we will explain in-depth when commenting the results shown in Tables 4.10 and 4.11.

Table 4.5 Settings for defining the pressure contour plots in Fig. 4.13, 4.14 and 4.15.

PRESSURE	Maximum [Pa]	322
	Minimum [Pa]	-581
CONTOURS	Nº of contours	50

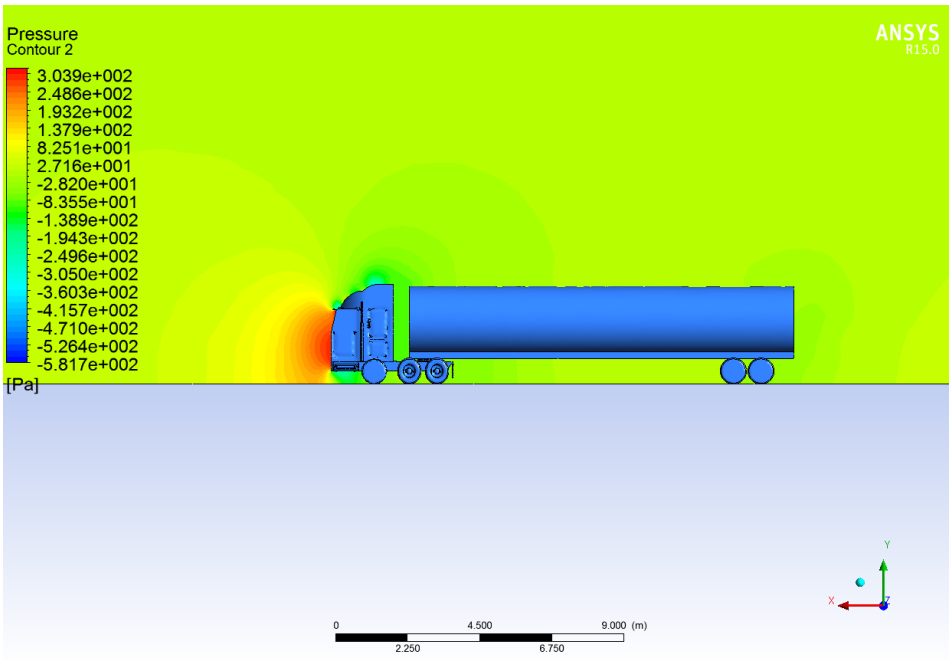

Fig. 4.13 Pressure contours for conventional diesel tanker truck in plane x=0 m.

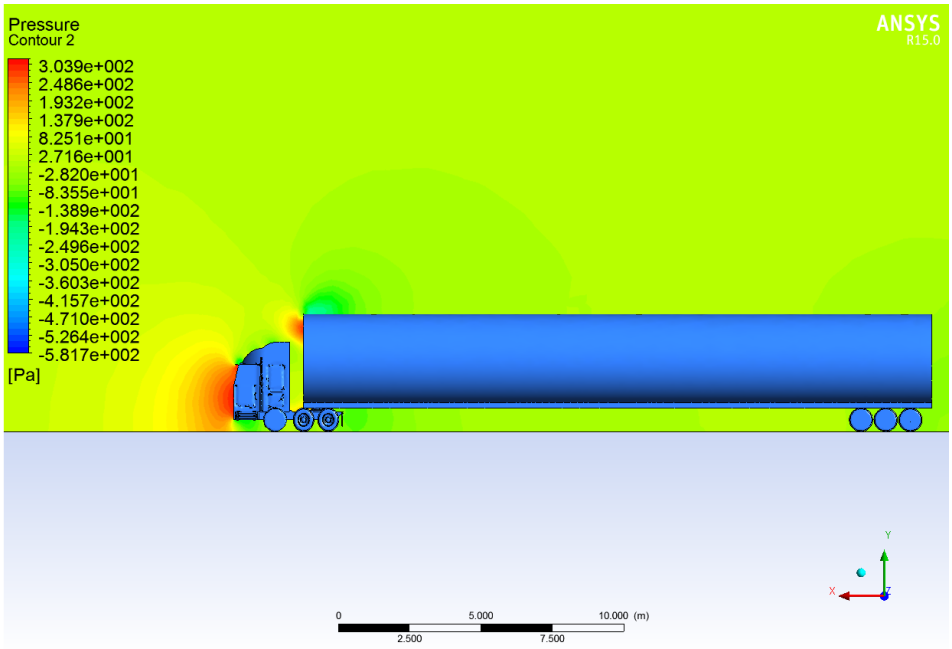

Fig. 4.14 Pressure contours for hydrogen fuel tanker truck with a single tank in plane x=0 m.

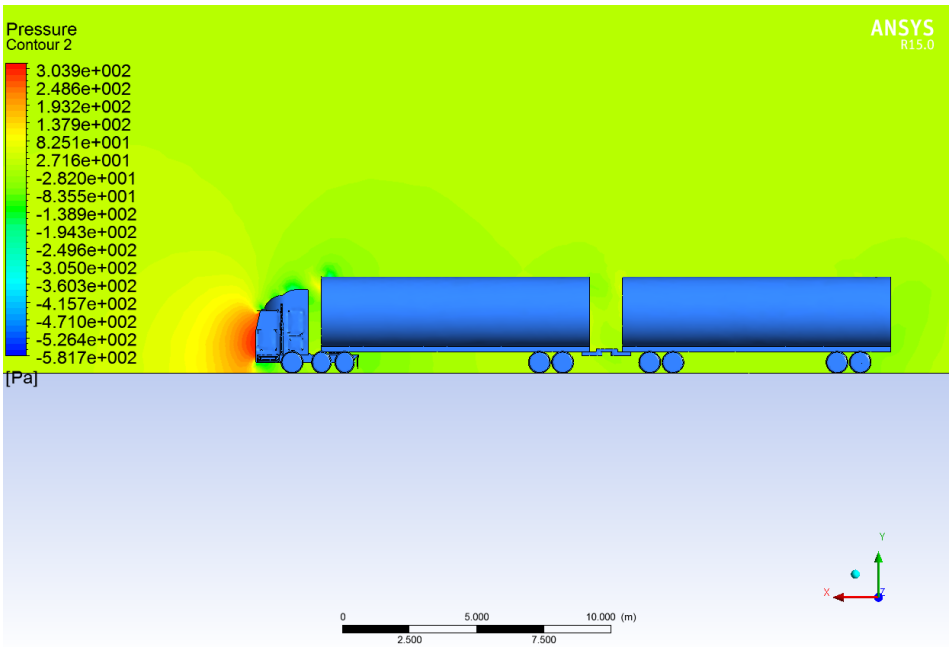

Fig. 4.15 Pressure contours for hydrogen fuel tanker truck with double tank (articulated truck) in plane x=0 m.

Fig 4.16, 4.17 and 4.18 show isometric views of the pressure contours on the surfaces of a conventional diesel tanker truck, and hydrogen fuel tanker trucks with a single tank and double tank, respectively. From these results, we can also see clearly what we explained before in relation to the height of the various tanks. These will be explained in-depth when commenting the results shown in Tables 4.10 and 4.11.

Table 4.6 Settings for defining the pressure contour plots in Fig. 4.16, 4.17 and 4.18.

PRESSURE	Maximum [Pa]	322
	Minimum [Pa]	-581
CONTOURS	Nº of contours	30

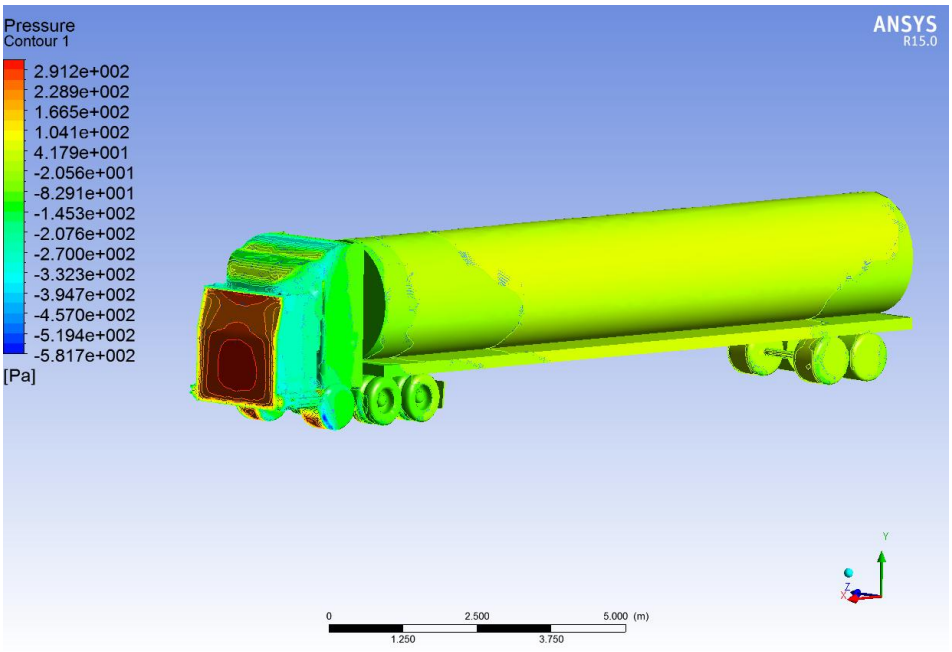

Fig. 4.16 Isometric view of pressure contours on the surface for conventional diesel tanker truck.

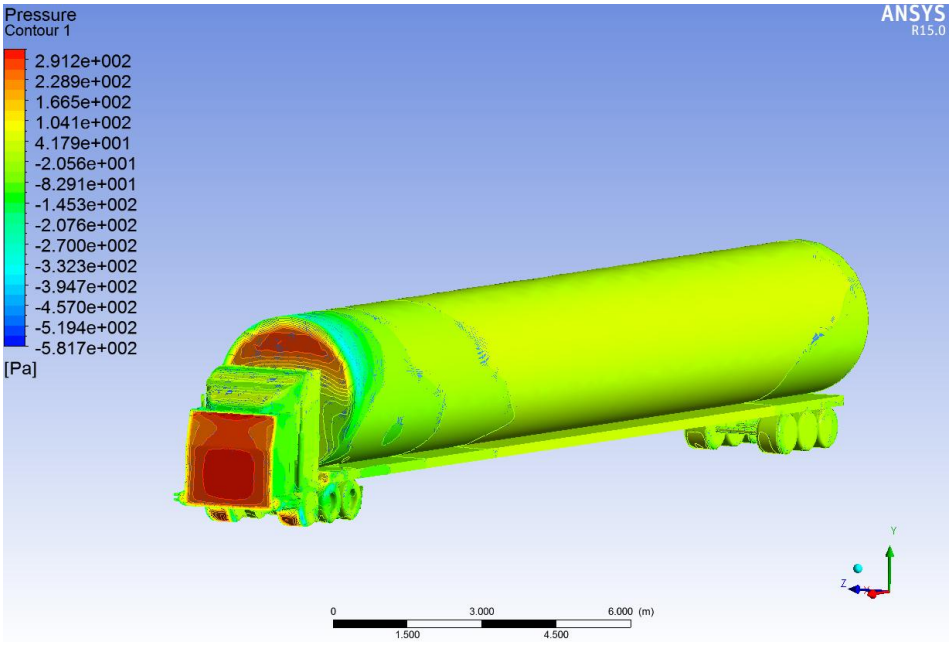

Fig. 4.17 Isometric view of pressure contours on the surface for hydrogen fuel tanker truck with a single tank.

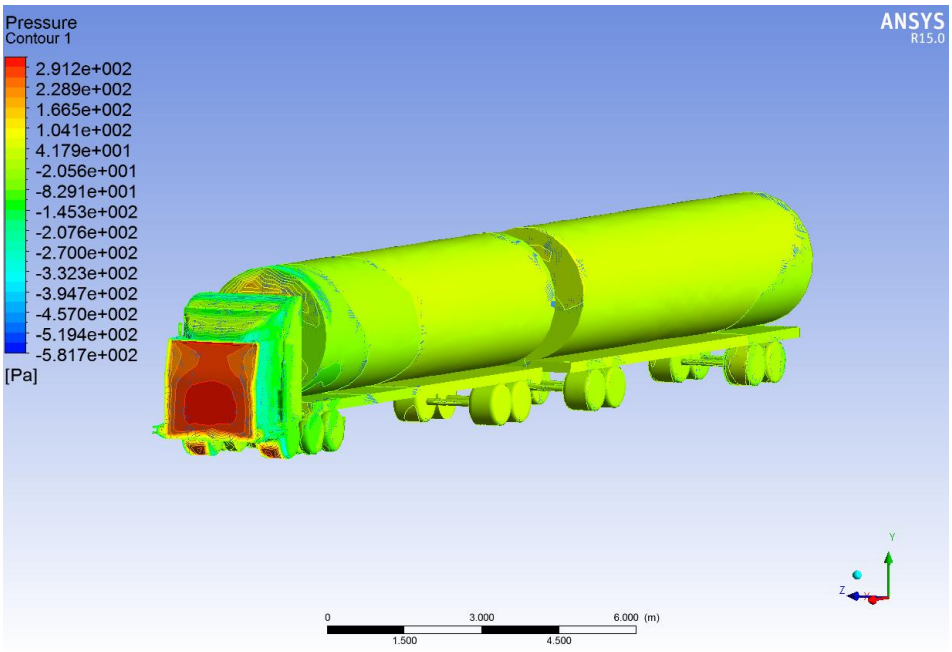

Fig. 4.18 Isometric view of pressure contours on the surface for hydrogen fuel tanker truck with double tank.

4.2. Numerical results.

4.2.1. Aircraft

The results shown in Tables 4.7, 4.8 and 4.9 were extracted from the simulations with ANSYS Fluent. The lift coefficient increases 2.65% in the aircraft with the hydrogen tank respect to the conventional A320. Although this may seem unexpected a priori, since both aircrafts have equal wings, we think that the lift coefficient might have increased due to the "lifting body" effect (the fuselage has a higher, positive contribution to the lift generated by the wing) and/or that the interference fuselage-wing for the modified aircraft is more beneficial to the lift generated by the wing than for the conventional A320. The lifting body effect appears when the fuselage, due to its shape, is also capable of producing significant lift. In this case, the shape of the fuselage for the modified A320 resembles that of lifting body aircraft concepts and that is way fuselage may be able to produce more lift than for the conventional A320.

Table 4.7 Lift and drag coefficients and aerodynamic efficiency (lift-to-drag ratio) for the studied aircraft configurations.

PARAMETER	CONVENTIONAL A320	MODIFIED A320	INCREMENT
C_L	0.11416	0.11719	2.65%
C_D	0.04761	0.05059	6.26%
E	2.40	2.32	-3.39%

If we want to know the induced drag contribution we have to compute it theoretically because ANSYS Fluent is not able to compute the induced drag. Therefore, recalling chapter 2, the induced drag will be:

$$k = \frac{1}{\pi \cdot 9.39 \cdot 0.92} = 0.03685$$

Hence,

$$C_{D_i}(\text{conventional A320}) = 0.03685 \cdot \ 0.11416^2 = 4.802 \cdot 10^{-4}$$

$$C_{D_i}(\text{modified A320}) = 0.03685 \cdot \ 0.11719^2 = 5.060 \cdot 10^{-4}$$

Table 4.8 Parasitic drag, induced drag and total drag coefficients for the studied aircraft.

TYPE OF DRAG	CONVENTIONAL A320	MODIFIED A320	INCREMENT
$\boldsymbol{C_{D_0}}$	0.04713	0.05009[3]	6.26%
$\boldsymbol{C_{D_i}}$	0.00048	0.00050	4.16%
$\boldsymbol{C_D}$	0.04761	0.05059	6.26%

Table 4.9 Pressure drag and viscous drag (or air friction drag) coefficient contributions to parasitic drag coefficient for the studied aircraft configurations.

TYPE OF DRAG	CONVENTIONAL A320	MODIFIED A320	INCREMENT
$\boldsymbol{C_p}$	0.03465	0.03593	3.70%
$\boldsymbol{C_f}$	0.01010	0.01466	45.1%
$\boldsymbol{C_{D_0}}$	0.04761	0.05059[4]	6.25%

In Chapter 2, it was shown that the total drag has two main contributions: parasitic drag and induced drag. Table 4.8 shows that these sources of drag increase 6.26% and 4.16%, respectively, for the modified aircraft compared to the conventional A320. Recalling again Chapter 3, the parasitic drag is composed of pressure drag, viscous drag and wave drag. On one hand, considering that in this study the aircraft was assumed to fly at Mach 0.78, wave drag is likely to be a small contribution because we are quite far from the supersonic regime. Thus, the regions of the fluid domain where the flow speed exceeds 311m/s (i.e., the speed of the sound at altitudes of 11 km for the ISA atmosphere) are not very significant (see Fig. 4.9 and Fig. 4.10), and the speeds there are close to 311 m/s, such that the shockwaves are of lowest intensity.

[3] C_{D_0} was calculated theoretically. The induced drag was calculated considering a value of e of 0.92 and AR of 9.39.

[4] Note that C_{D_0} is equal to C_D because ANSYS Fluent is not able to calculate C_{D_i}.

On the other hand, the pressure drag and viscous drag increase 3.70% and 45.1%, respectively, for the modified aircraft compared to the conventional A320. The increase in the pressure drag is an expected result because the aircraft with hydrogen tank is a vehicle less streamlined and has larger frontal area and therefore a larger turbulent wake appears.

The increase in viscous drag or skin friction drag is also expected because the wet area for the modified aircraft is significantly larger compared to the conventional A320, that is, there is much more contact area between the fluid and the aircraft surface where friction can act. What is not as expected, though, is the fact that the skin friction drag is in both cases smaller than the pressure drag.

Normally, for streamlined vehicles like commercial civil aviation aircraft, the viscous drag is dominant because the wet area is very large compared to the frontal area.

Induced drag; is associated with the vortices generated in the wing tips when the wing is generating lift, which appear due to the higher pressure of the air in the intrados compared to the extrados in a normal flight condition with positive lift.

The energy necessary to create these vortices (kinetic energy to the air for it to acquire rotational/tangential velocity component) is provided by the aircraft and therefore, fuel is wasted in generating these vortices, an undesired consequence of generating lift that is not useful to flight.

Hence, since a particular aircraft's required lift is set by its weight. If, for a given payload and fuel mass, the modified A320 has larger mass due to the increased structural mass associated with the larger tank, since they both have equal wing, it will have to fly with increased angle of attack and thus increased induced drag, unless this is compensated by the fact that the modified A320 is a little better generating lift, as seen in Table 4.7.

Finally, the aerodynamic efficiency, or lift-to-drag ratio decreases 3.39%. This means that, while the modified aircraft may be better at generating lift, this is counterbalanced by a comparatively higher increase in drag. This is very important because a lower efficiency implies lower fuel economy and climb and glide performances, etc.

4.2.2. Tanker truck

Table 4.10 shows the lift and total drag coefficients for the studied truck configurations. What is really interesting in this study is the total drag coefficient. The total drag coefficient increases 19.1% and 29.2%, respectively, for the hydrogen fuel tanker trucks with single tank and double tank, both compared to the conventional diesel tanker truck.

To better understand these increments of drag, Table 4.11 shows the contribution of the pressure drag and viscous drag coefficients tot total drag. As

we can see, the value of pressure drag is much larger than the viscous drag. This is as expected, since, normally, for non-streamlined (blunt) vehicles like cars, vans and trucks, the pressure drag is dominant because the frontal area is very large compared to the wet area.

Table 4.10 Drag coefficients for the studied tanker truck configurations.

PARAMETER	DIESEL TANK	SINGLE HYDROGEN TANK	DOUBLE HYDROGEN TANK
C_D	0.5139	0.6122	0.6640
INCREMENT		19.1%	29.2%

Table 4.11 Pressure drag and viscous drag (or air friction drag) coefficient contributions to parasitic drag coefficient for the studied tanker truck configurations.

TYPE OF DRAG	DIESEL TANK	SINGLE HYDROGEN TANK	DOUBLE HYDROGEN TANK
C_p	0.4960	0.5854	0.6276
C_f	0.0178	0.0268	0.0363
C_{D_0}	0.5139	0.6122	0.6640
C_p **INCREMENT**		18%	26.5%
C_f **INCREMENT**		49.9%	103.6%
C_{D_0} **INCREMENT**		19.1%	29.2%

Finally, the hydrogen fuel tanker trucks with single tank and double tank show a considerable increase in the viscous drag with respect to the conventional diesel tanker truck. The reason is because, as explained before, in order to store an amount of hydrogen fuel that has en equivalent level of overall energy, we had to increase the size of the fuel tank(s) due to the lower density of hydrogen. Thus, the wet area increases significantly for the hydrogen fuel tanker trucks with single tank and double tank, compared to the conventional diesel tanker truck. Moreover, since for the former trucks, the tanks are higher than the cabin of the truck, they also create more pressure drag.

4.3. Implications in fuel consumption for the modified A320.

In this section, the increment of fuel needed to fly the A320 with the hydrogen fuel tank due to its the larger fuel tank compared with the conventional A320 is computed.

We have seen in previous sections that when flying in horizontal flight, like typically in the, cruise phase, the forces are balanced (see Fig. 2.2) so we can deduce the following expression:

$$T = D = \frac{1}{2}\rho S V^2 C_D$$

Besides, we have seen that the total drag coefficient varies depending on the vehicle under study. Hence, the thrust will be different in each case. Assuming that S, V^2 and ρ are constant and equal for both aircraft (which is valid since we assume that both fly in the same cruise conditions of speed and altitude, and both have the same wing layout),Table 4.12, shows the thrust depending on the total drag coefficient:

Table 4.12 Thrust depending on total drag coefficient.

AIRCRAFT	TOTAL DRAG COEFFICIENT	THRUST [N]
CONVENTIONAL A320	0.0476186	56207
HYDROGEN A320	0.050598	59724

Considering that the Thrust Specific Fuel Consumption (TSFC) is also constant because we have not changed the engines of the aircraft, in order to provide more thrust we have to increase the Fuel Flow (FF) as follows.

$$FF = TSFC \cdot T$$

Table 4.13 shows the FF needed for each case of study.

Table 4.13 Fuel flow depending on thrust requirements.

AIRCRAFT	TSFC[kg/(N·s)]	FF[kg/s]
CONVENTIONAL A320	0.000016	0.90
MODIFIED A320	0.000016	0.96

From now on, we have an idea about the extra fuel that would be burnt due to having a larger fuel tank that affects the aerodynamics of the vehicle. As said in previous sections, contrary to kerosene, the combustion of hydrogen does not emit GHG. Therefore, a higher extra fuel burnt does not imply any controversial effect to the environment since hydrogen is an eco-friendly fuel.

However, the operational range can be affected due to burning fuel faster than before. The actual operational range of an A320 aircraft is of 6100 km with a maximum fuel capacity of 27200 L. Hydrogen will be stored in a liquid phase because of the reasons mentioned in previous sections. Recalling Chapter 1, Table 1.1 shows a comparison between hydrogen and Jet-A1 properties. Table 4.14 shows the A320 aircraft performances to better understand the problem.

Table 4.14 Airbus A320 aircraft performances.

MAXIMUM RANGE [Km]	TIME SPENT TO FLY THE MAXIMUM RANGE [s]	ENGINES X2	MAX FUEL CAPACITY [L]
6100	26521	CFM56-5B	27200

To flight a distance of 6100 km, which is the maximum operational range for an Airbus A320, we have to release a total amount of energy of:

$$\text{Released energy/range } = 22304\ kg\ JetA \cdot 42.8\ \frac{MJ}{kg} = 954611.2\ MJ$$

Assuming that we want to keep the operational range, the kilograms of hydrogen needed without any structural modification of the vehicle are:

$$kg \text{ of } H_2 \text{ (no structural change)} = \frac{954611.2\ MJ}{141.9\ \frac{MJ}{Kg}} \approx 6727\ kg$$

However, as seen in previous sections, hydrogen occupies a higher volume than Jet A. We saw that due to the higher fuel tank to store hydrogen the aerodynamics of the aircraft are modified, increasing the drag. In particular, the drag has increased 6%. Therefore, when involving the aerodynamics issue, the kilograms needed to fly the maximum range is:

$$kg \text{ of } H_2 \text{ (structural change)} = 6727.35\ kg \cdot 1.06 \approx 7131\ kg$$

Now, we know the kilograms of hydrogen and Jet A needed to achieve this range. Hence, we are able to analyze the economic impact. Table 4.15 shows the price of Jet A and hydrogen in a liquid phase.

Table 4.15 Price of Jet A and Hydrogen in a liquid phase.

JET-A [€/L]	HYDROGEN [€/kg]
0.37	4.7

The cost of flying the maximum range with Jet-A or Hydrogen for an airline is:

$$\text{Jet} - \text{A cost} = 0.37 \cdot 27200 = 10064\ €$$

$$\text{Hydrogen cost} = 4.7 \cdot 7131 = 33515.7\ €$$

We can see that flying with hydrogen as fuel is much more expensive, in particular, the cost is 23451.50 € higher. The reason is that, at present day, the production of hydrogen is much more expensive. As we have seen in Chapter 1, the hydrogen production process requires many phases which have to be carefully controlled. Therefore, to decrease the cost of production of hydrogen,

the technology and logistics involved have to improved, and hopefully this will be achieved in the short-term future.

The purpose of implementing hydrogen as fuel is that is an eco-friendly fuel and this may compensate for the extra cost. To show that, the chemical combustion process is shown below:

$$2H_2 + O_2 \rightarrow 2H_20$$

As we can see, only water vapour is produced so no GHG are emitted. On the other hand, the combustion process of kerosene is:

$$2C_{12}H_{26} + 37O_2 \rightarrow 26H_2O + 24CO_2$$

As a result of the combustion process we obtain water vapour and dioxide of carbon which is a GHG, and therefore it pollutes. Specifically, we have said that we need 22304 Kg of kerosene to cover a distance of 6100 km. With the CO_2 calculator provided by Nature Fund [30], to travel a distance from Barcelona to New York which is approximately 6100 km we emit 2.339 kg of CO_2 per flight.

4.3.1. Structural problem.

In this section we will be more accurate and we will compute the range of the modified aircraft considering the structure of the hydrogen fuel tank. Since both aircrafts have the same wing, if the lift is not able to compensate the total weight of the aircraft considering the weight of the structure, the aircraft will have to fly with a higher angle of attack to generate more lift and thus increased induced drag will appear.

At present day, the majority of aircrafts are made of aluminium alloys [31]. However, aircraft manufacturers are involving composite materials with a huge effort because of their advantages [32]. We will compute the added weight due to the structure considering that is made of an aluminium alloy; its density is of 2700 kg/m^3.

In chapter 3, we designed the new fuel tank as an ellipse. We want to compute the volume of the fuel tank. The perimeter of the ellipse can be computed with the formula bellows:

$$P \approx 2\pi \sqrt{\frac{a^2 + b^2}{2}}$$

Where a is the major axis and b the minor axis of the ellipse.

Knowing that the longitude of the fuel tank is of 18.71 m, the total area is of 160.72 m^2. To compute the volume we need the thickness. Usually, the thickness is of 1-1.5 mm, but as we will have other elements to step up the

structure and they affect the total weight, we will consider a thickness of 2 mm. Hence, the total volume will be of 0.32 m^3 and the mass due to the structure is:

$$M_1 = 0.32 \cdot 2700 \approx 867\ kg$$

In order to know which is the difference between the weight of including or excluding the fuel tank, we also need to know the structural mass before including the fuel tank. To compute it, we procedure as follows:

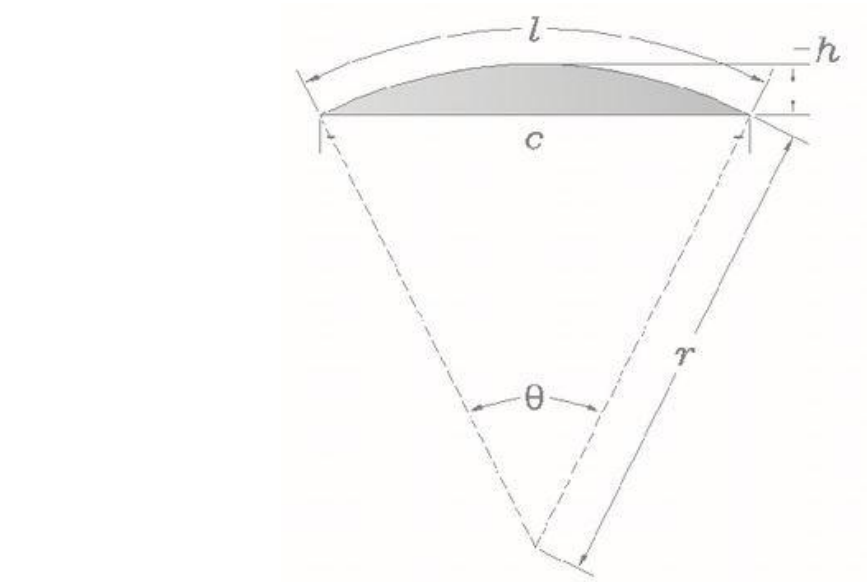

Fig. 4.19 Scheme of the circular segment.

Where l is the length, c the chord, $\theta$the angle, r the radius and h the height.

To compute the length,

$$l = \alpha R = 122 \cdot \frac{\pi}{180} \cdot 1.975 = 4.2\ m$$

And therefore, the total area, volume and mass are:

$$A = l \cdot longitude = 4.2 \cdot 18.71 = 78.88\ m^2$$

$$V = A \cdot thickness = 78.88 \cdot 0.002 = 0.157 m^3$$

$$M_2 = 0.157 \cdot 2700 \approx 426\ kg$$

Hence, the added weight due to the hydrogen fuel tank is:

$$M_1 - M_2 = 867 - 426 = 441\ kg$$

$$W = (M_1 - M_2) \cdot g = 4335.26\ N$$

Since the difference between the lifts of the conventional A320 and modified hydrogen is of 3577 N (see Table 5.2), we can conclude that we have to flight

we a higher angle of attack because we are not able to compensate the added weight with the current lift. Therefore, a higher angle of attack will involve an increase of the induced drag. Otherwise, hydrogen weights less than Jet-A fuel so when including the fuel in the aircraft, we have:

$$W_{A320,Jet-A} = (22304 + 441) \cdot g = 222901\ N$$

$$W_{A320,Hydrogen} = (6727.352 + 867) \cdot g = 74424.64\ N$$

And therefore, we are able to compensate the exceeding lift.

4.4. Implications in fuel consumption for the tanker truck.

As happened in the case of the aircraft we have an increase of drag and its correspondent increase of thrust. This growth implies more fuel consumption per kilometre. To calculate the reduction of range and the increase of fuel keeping the same range we followed the same steps as in the aircraft, in this case we are only going to present the results.

Table 4.16 Range and cost between each type of tanker truck.

	Diesel tanker truck	**One hydrogen tank tanker truck**	**Double hydrogen tank tanker truck**
Range [Km]	3947.36	3193.42	2794.73
Diesel needed to do 3947.36 Km [Kg]	1248	1486.36	1612.41
Entire tank cost [€]	1725	2054.47	2228.7

We can compute now the structural gain of weight and the amount of weight we save in terms of fuel.

Table 4.17 Weight differences between each type of tanker truck.

	Diesel tanker truck	**One hydrogen tank tanker truck**	**Double hydrogen tank tanker truck**
Tank weight [Kg]	504.15	1265.57	952.66
Fuel weight [Kg]	33280	11894.4	8127.84
Weight difference [%]		-4.09	-28.49

CHAPTER 5. WIND TUNNEL TESTS

In this chapter, we will analyze with wind tunnel experiments the aerodynamic performances of mock-up models of the conventional A320 and the modified aircraft, to compare the results with those from the CFD simulations done previously, as reported in Chapter 4.

First, the CAD models of the studied aircraft were printed with a 3D printer.

Second, before testing the 3D models in the wind tunnel, we have to prepare them. The models were puttied with polyester putty. After the putty had dried, the models were polished and painted with white acrylic spray. A support handle was made to attach the aircraft models to the 3-component scale and hold them in the test chamber of the wind tunnel.

The models were placed as centered as possible within the test chamber (see Fig. 5.1 and Fig. 5.2). Note that null or very small angle of attack was provided to the models because we are supposing that both aircrafts are flying in cruise phase, where angles of attack are very small due to the high cruise speed.

We were also compliant with wind tunnel testing recommendations, stating that, the model wing span (27 cm) must not be larger than 80% of the width of the test chamber (40 cm), and that the frontal area of the models (around 0.0045 m^2) must not be greater than 10% of the test chamber frontal area (0.16 m^2). These considerations ensure that the flow around the model behaves as if there were no test chamber walls and the models were flying in open atmosphere, that is, such that presence of these walls does not disrupt the aerodynamic performance results.

There are different ways for measuring the aerodynamic forces, for instance, by means of static pressure ports all over the surface, we can compute the pressure distribution and, with this, the lift and lift coefficient; and the flow velocity profile downwind is directly linked to the aerodynamic drag on the model. In our case, making static pressure ports in our models was very complex and troublesome. Thus, we measured the lift and the drag directly with the 3-components scale or 3-axes scale. The results are shown in Table 5.1

Table 5.1 Lift and drag coefficients and efficiency results for the wind tunnel aircraft study.

PARAMETER	CONVENTIONAL A320	MODIFIED A320	INCREMENT
C_L	0.19206	0.15850	-21.17%
C_D	0.07185	0.07754	7.91%
E	2.67	2.04	-30.88%

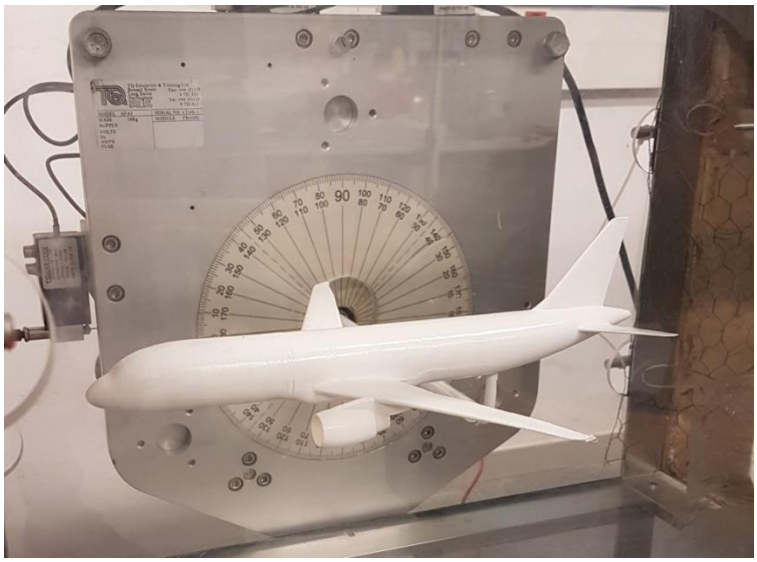

Fig. 5.1 Conventional A320 3D model inside the test chamber of the wind tunnel.

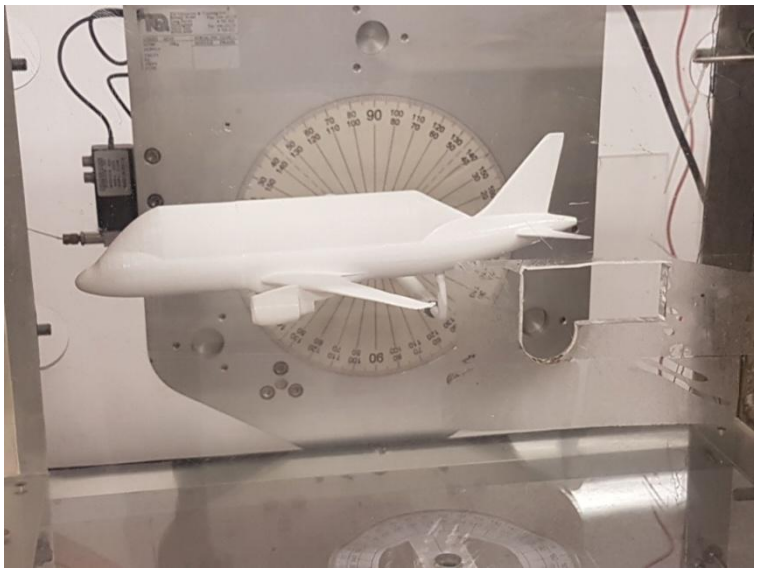

Fig. 5.2 Modified A320 model inside the test chamber of the wind tunnel.

Obvious differences can be seen when comparing the results from the wind tunnel tests with the obtained from the CFD simulations (see Table 5.2). The results of the wind tunnel tests may show error due to issues, such as the smoothness of the 3D model, the alignment with the flow, etc. To clearly see the error between the results of the CFD simulations and the wind tunnel tests, we made another CFD simulation replicating the fluid problem corresponding to the wind tunnel test for the conventional A320 model. Fig. 5.2 shows contours plots for the static pressure for this latter simulation.

Table 5.2 Lift, aerodynamic drag and efficiency as obtained from the CFD simulations for the full-scale aircraft in cruise conditions.

PARAMETER	CONVENTIONAL A320	MODIFIED A320	INCREMENT
C_L	0.11416	0.11719	2.65%
C_D	0.04761	0.05059	6.26%
E	2.40	2.32	-3.39%

Table 5.3 Wind tunnel CFD simulation data.

REFERENCE VALUES	Area [m^2]	0.0045
	Density [kg/m^3]	1.225
	Gauge pressure [Pa]	0
	Velocity [m/s]	33.33
	Viscosity [kg/m·s]	$1.81x10^{-5}$

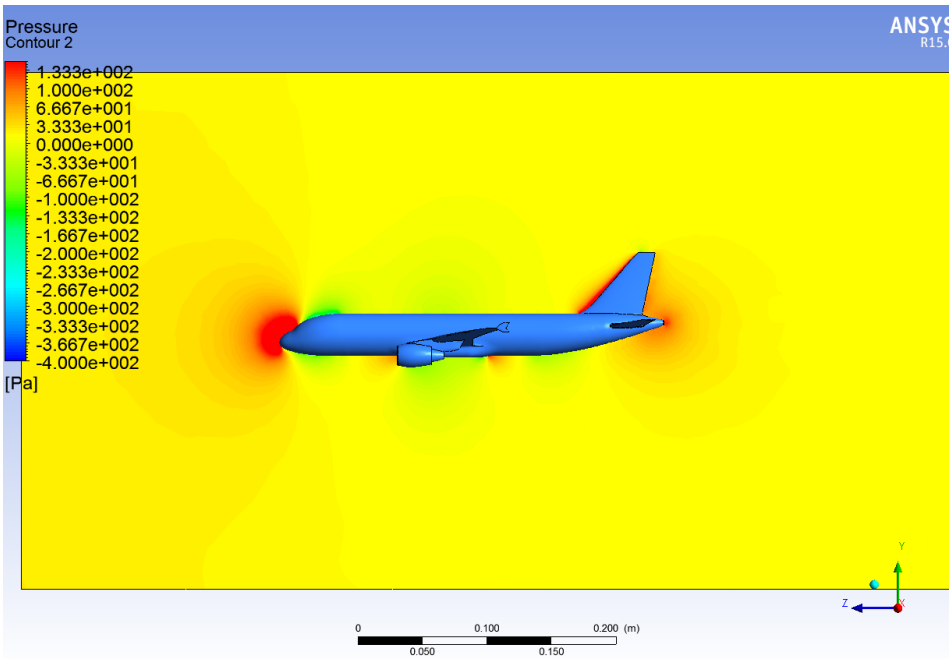

Fig. 5.3 Pressure contours in plane x=0 m for the CFD simulation of the conventional A320 aircraft model in wind tunnel test.

Table 5.4 Lift and aerodynamic drag coefficients, and efficiency, as obtained from a CDF simulation, imitating the wind tunnel test conditions for the conventional A320.

PARAMETER	CONVENTIONAL A320	MODIFIED A320	INCREMENT
C_L	0.42	0.34661	-21.17%
C_D	0.384	0.41439	7.91%
E	1.09	0.83	31.32%

Comparing this simulation with Fig. 4.3 of the other simulation, we can observe that the behaviour of the aircraft is the same but the values of pressure and aerodynamic coefficients are different. This difference can be reduced with the appropriate scale factor from the wind tunnel test results.

5.1. Prandtl-Glauert transformation.

The purpose of this section is to apply correction factors to the drag and lift coefficients obtained from the wind tunnel tests in order to obtain the real lift and drag coefficients for the conventional A320 and modified aircraft. The correction factor in each case will be obtained from the Prandtl-Glauert transformation theory.

The Prandtl-Glauert theory states that drag and lift coefficients are affected by the next factor:

$$\alpha = \frac{1}{\sqrt{1 - M^2}}$$

Fig. 5.4 shows the behaviour of the lift coefficient depending on the Mach number described by the Prandtl-Glauert transformation theory.

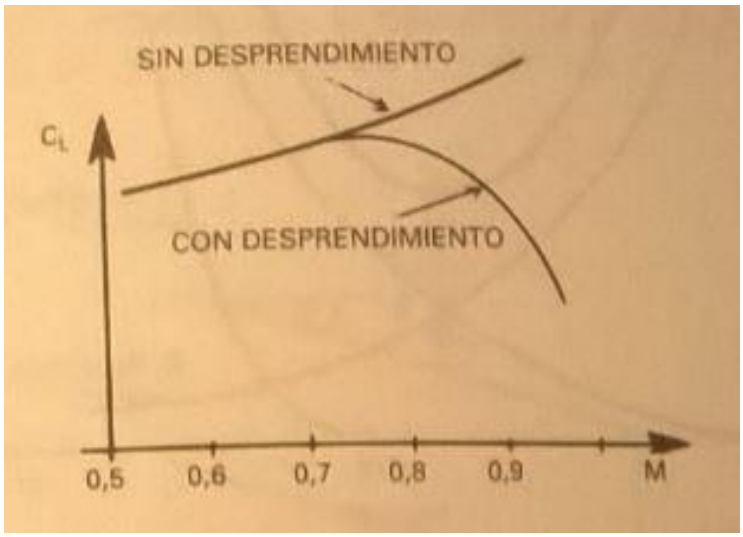

Fig. 5.4 Prandtl-Glauert theory. Lift and drag coefficients with Mach dependency.

Fig.5.4 shows that until a certain value of Mach (where compressibility effects start to appear), lift and drag coefficients increase while Mach also increases. Therefore, we are able to compute the α factor for the real situation and for the aircraft model tested in the wind tunnel.

$$\alpha_{real} = \frac{1}{\sqrt{1 - M_{real}^2}} = 1.598$$

$$\alpha_{model} = \frac{1}{\sqrt{1 - M_{model}^2}} = 1.005$$

In that way, we can obtain the increment between the factors which is 59%. Now, this correction factor has to be applied to all drag and lift coefficients obtained from the wind tunnel tests. Table 5.5 shows all drag and lift coefficients for the conventional A320 and modified aircraft with the correction factor applied.

Table 5.5 Drag and lift coefficients corrected due to the Prandtl-Glauert transformation.

PARAMETER	CONVENTIONAL A320	MODIFIED A320
C_L	0.30543	0.25206
C_D	0.11426	0.12331

CHAPTER 6. CONCLUSIONS AND FUTURE WORK

Nowadays, 90% of worldwide vehicles work with fossil fuels, increasing the pollution and GHG. Hydrogen has been suggested as a possible alternative. It is very interesting due to its high specific energy, and because its combustion does not emit GHG, and so it would contribute to mitigate the global warming. However, due to its lower energy density, hydrogen requires fuel tanks with larger volume than conventional fuels, for an equivalent amount of energy released. The larger tanks modify the external geometry of the vehicle and therefore the aerodynamics are also different.

In this project, we conducted an experimental and CFD analysis of an Airbus A320 and a tanker truck for which the geometries have been modified accounting for the larger hydrogen fuel tanks needed. The analysis was carried out learning about the hydrogen properties, how to deal with ANSYS Fluent software and wind tunnel testing, and performing a CFD analysis on each vehicle.

The CAD designs of the modified vehicles were performed trying to design a tank that would be able to store an equivalent amount of energy. Besides, to study the implementation of hydrogen in tanker trucks, a single hydrogen tank tanker truck and a double hydrogen tank tanker truck were created trying to be compliant with the Spanish laws for trucks.

With CFD simulations, we obtained de drag and lift coefficients for the aircraft and the drag coefficient for the tanker truck. The lift coefficients obtained were 0.11416 and 0.11719 for the conventional A320 and modified aircraft respectively. The drag coefficients obtained were 0.04761 and 0.05059 respectively too. Talking about the tanker truck study, the drag coefficients obtained were 0.5139 for the diesel tanker truck, 0.6122 for the one single hydrogen tank tanker truck and finally 0.6640 for the double tank tanker truck. Furthermore, pressure contour plots and velocity contour plots were obtained to see graphically the behaviour of the fluid flow around the vehicles. In the modified A320, the hydrogen tank is responsible of generating more drag; particularly, on one side, the wet area increases and so it also increases the friction drag. On the other side, the tank generates an abrupt detachment of the flow in its rear-most corner, and therefore a turbulent wake is created, causing a pressure unbalance, and consequently more pressure or wake drag. Surprisingly, the overall lift for the A320 also increased, maybe due to a lifting body effect.

As per the tanker trucks, both studied designs present an increase of the total drag. This is expected because we had to increase the size of the fuel tank(s) due to the lower energy density of hydrogen, and thus the wet area increases significantly

We studied also how much fuel we needed to burn to produce thrust and overcome the new total drag caused by the existence of the hydrogen tank. We had to take some factors into account such as the new weight of the additional structure to store the hydrogen and the total amount of fuel we are carrying.

Only talking about the structure, there is an expected weight increment and for this reason, in the aircraft case we need to generate more lift and in the truck case we have to give more thrust. However, the structure is not the only weight that changes. Because of the lower energy density, the weight of hydrogen we are carrying decreases, allowing us to keep the same performances in both cases.

As we said previously, the increment of fuel that we carry to keep the same equivalent energy is translated into an extra cost. Nowadays, hydrogen is very expensive compared with Jet Fuel or Diesel fuel. Thus, the kilometres travelled would be more expensive and also the boarding pass prices.

Finally, we printed the aircraft CAD designs in a 3D printer provided by the university. The main idea was to test these 3D models in an open wind tunnel to obtain the experimental lift and drag coefficients and compare these results with those obtained from the CFD simulations. The results were compared also with a CFD simulation recreating the wind tunnel conditions to estimate the error between the CFD simulations and wind tunnel experiments. As there are many factors affecting both, it is often complicated to obtain exactly the same results. In any case, it can be seen that drag also increases 7.91% from the conventional A320 to the modified A320. Although lift does not increase like predicted by the CFD simulations, the aerodynamic efficiency also decreases -30.88% for the modified A320.

At the end of this project, it can be said that the main objective was accomplished: to study the impact (environmental, economical, etc.) of introducing hydrogen as fuel in an Airbus A320 and tanker truck.

We hope that hydrogen production and distribution technologies and logistics improve and therefore hydrogen price diminishes in the short-term future. As future work, to obtain more accurate results, CFD simulations could be carried out with a Large Eddy Simulation (LES) or Direct Numerical Simulation (DNS) method, the last one even more accurate. Obviously, the computational load and the time to perform the simulations will increase considerably. For that reason, a good cluster of computers would be a good solution. As we said before, the incident flow on the vertical stabilizer is turbulent and affected by the hydrogen tank. Hence, the aerodynamic forces that appear on the stabilizer and the moments generated by it will change respect to the conventional A320. CFD simulations would be needed in order to better comprehend the implications of this on aircraft yaw control.

Nowadays, the use of composites in airframes is increasing because their low density supposes large savings in fuel consumption for airlines. Introducing composites in the structure of the hydrogen tank would allow reducing the weight and thus the required thrust. In our case, the friction drag is an important problem for both modified vehicles. Thus, for example, research on nanopainting would help reducing the extra drag created by the hydrogen tank. Summing up, with nanopainting and composites, keeping the same volume of fuel, we may be able to increase the operational range beyond that of the current A320.

REFERENCES

[1] Faye. L & Jackson. NASA: Global Climate Change. California Institute of Technology, US. Available at: https://climate.nasa.gov/

[2] Satyapal. S. Office of Energy and Renewable Energy: Hydrogen production, natural gas reforming. Washington, US. Available at: Available at: https://energy.gov/eere/fuelcells/hydrogen-production-natural-gas-reforming

[3] Satyapal. S. Office of Energy and Renewable Energy: Electrolysis. Washington, US. Available at: Energy efficiency and renewable energy

[4] Satyapal. S. Office of Energy and Renewable Energy: Gasification of coal. Washington, US. Available at: https://energy.gov/fe/how-coal-gasification-power-plants-work

[5] Satyapal. S. Office of Energy and Renewable Energy: Hydrogen from biomass. Washington, US. Available at: https://energy.gov/eere/fuelcells/hydrogen-production-biomass-gasification

[6] Wade A. Amos. (1998). National renewable energy laboratory, costs of storing and transporting hydrogen [PDF file]. National Renewable Energy Laboratory. Recovered from http://www.nrel.gov/docs/fy99osti/25106.pdf.

[7] Wade A. Amos. (1998). National renewable energy laboratory, costs of storing and transporting hydrogen [PDF file]. National Renewable Energy Laboratory. Recovered from http://www.nrel.gov/docs/fy99osti/25106.pdf.

[8] Wade A. Amos. (1998). National renewable energy laboratory, costs of storing and transporting hydrogen [PDF file]. National Renewable Energy Laboratory. Recovered from http://www.nrel.gov/docs/fy99osti/25106.pdf.

[9] Wade A. Amos. (1998). National renewable energy laboratory, costs of storing and transporting hydrogen [PDF file]. National Renewable Energy Laboratory. Recovered from http://www.nrel.gov/docs/fy99osti/25106.pdf.

[10] Holman. J. Royal society of chemistry: Hydrogen. United Kingdom, EU. Available at: http://www.rsc.org/periodic-table/element/1/hydrogen

[11] US Department of Energy. (2014). Alternative Fuels Data Center – Fuel Properties Comparison [PDF file]. Energy efficiency and renewable energy. Recovered from http://www.afdc.energy.gov/fuels/fuel_comparison_chart.pdf

[12] U.S. Department of Energy Hydrogen Program. (2006). Technical Assessment: Cryo-Compressed Hydrogen Storage for Vehicular Applications (Rev. 1) [PDF file]. US Department of Energy. Recovered from https://www.hydrogen.energy.gov/pdfs/cryocomp_report.pdf.

[13] U.S. Department of Energy Hydrogen Program. (2006). Technical Assessment: Cryo-Compressed Hydrogen Storage for Vehicular Applications (Rev. 1) [PDF file]. US Department of Energy. Recovered from https://www.hydrogen.energy.gov/pdfs/cryocomp_report.pdf.

[14] M. W. Melaina, O. Antonia, and M. Penev. (2013). Blending Hydrogen into Natural Gas Pipeline Networks: A Review of Key Issues [PDF file]. National renewable energy laboratory. Recovered from http://www.nrel.gov/docs/fy13osti/51995.pdf

[15] ENGINEERING TOOLBOX. Laminar, transitional and turbulent flow Available at: http://www.engineeringtoolbox.com/laminar-transitional-turbulent-flow-d_577.html

[16] MIT. (2006). Course notes on aerodynamics 2006 (revised on 2009) [PDF file]. MIT. Recovered from: http://web.mit.edu/snively/www/2_006%20Coursenotes.pdf

[17] European Organisation for the Safety of Air Navigation, International Civil Avioation Organization, and the Flight Safety Foundation. Skybrary: Form drag. Available at: http://www.skybrary.aero/index.php/Friction_Drag

[18] Mellibovsky, F.*Thrust equations, Aerospace Science & Technology,* pp.

[19] H. Nancy. NASA: Types of wind tunnels. California Institute of Technology, US. Available at: https://www.grc.nasa.gov/www/k-12/airplane/tuntype.html

[20] Frank M. White. (2003). Fluid mechanics “Principle of Dynamic Similarity” (5th edition). Editorial McGraw-hill.

[21] REPSOL, Características combustible Jet A-1. Available at: https://www.repsol.com/es_es/productos-servicios/aviacion/productos/jet-a-1/

[22] Sclar. D. DUMMIES: The pros and cons of diesel engines. Available at: http://www.dummies.com/home-garden/car-repair/diesel-engines/the-pros-and-cons-of-diesel-engines/

[23] U.S. Energy Information Administration: How much carbon dioxide is produced by burning gasoline and diesel fuel? Available at: http://www.eia.gov/tools/faqs/faq.cfm?id=307&t=11

[24] College of the Desert. (2001). Hydrogen Fuel Cell Engines and Related Technologies (Rev. 0) [PDF file]. Energy Technology Training Center Recovered from http://infohouse.p2ric.org/ref/45/44490.pdf

[25] Felipe. A. El Economista: La DGT da luz verde al uso de los megacamiones en España. Available at: http://www.eleconomista.es/transportes/noticias/7560493/05/16/La-DGT-da-luz-verde-al-uso-de-los-megacamiones-en-Espana.html

[27] Área de formación y comportamiento de conductores. (2011). Reglamentación sobre vehículos pesados, prioritarios, especiales, de transporte de personas y mercancías y tramitación administrativa [PDF file]. DGT Recovered from: http://www.dgt.es/Galerias/seguridad-vial/formacion-vial/cursos-para-profesores-y-directores-de-autoescuelas/doc/XIV_Curso_26_ReglamentacionVehPesados.pdf

[28] ANSYS Fluent User's Guide: Evaluation of Gradients and Derivatives. Available at: https://www.sharcnet.ca/Software/Fluent6/html/ug/node994.htm

[29] Olmo. M & Nave. R. HYPERPHYSICS: Ecuación de Bernoulli. Available at: http://hyperphysics.phy-astr.gsu.edu/hbasees/pber.html

[30] Nature Fund: Emisión de dióxido de carbono a través un viaje en avión. Available at: http://www.naturefund.de/es/tierra/calculador_de_co2/calculador_de_co2_avion.html

[31] Ontiveros. J. HISPAVIACON: El avion y su diseño, fabricacion y mantenimiento. Available at: http://www.hispaviacion.es/el-avion-diseno-fabricacion-y-mantenimiento-2/

[32] AIMPLAS: Los composites en el sector aeronáutico. Available at: http://www.aimplas.es/blog/los-composites-en-el-sector-aeronautico